

# Calibration of White Dwarf cooling sequences: theoretical uncertainty

Pier Giorgio Prada Moroni

*Dipartimento di Fisica Università di Pisa, 56127 Pisa, Italy*

*INFN, Sezione di Pisa, 56010 Pisa, Italy*

*Osservatorio Astronomico di Collurania, 64100 Teramo, Italy*

and

Oscar Straniero

*Osservatorio Astronomico di Collurania, 64100 Teramo, Italy*

## ABSTRACT

White Dwarf luminosities are powerful age indicators, whose calibration should be based on reliable models. We discuss the uncertainty of some chemical and physical parameters and their influence on the age estimated by means of white dwarf cooling sequences. Models at the beginning of the white dwarf sequence have been obtained on the base of progenitor evolutionary tracks computed starting from the zero age horizontal branch and for a typical halo chemical composition ( $Z=0.0001$ ,  $Y=0.23$ ). The uncertainties due to nuclear reaction rates, convection, mass loss and initial chemical composition are discussed. Then, various cooling sequences for a typical white dwarf mass ( $M=0.6 M_{\odot}$ ) have been calculated under different assumptions on some input physics, namely: conductive opacity, contribution of the ion-electron interaction to the free energy and microscopic diffusion. Finally we present the evolution of white dwarfs having mass ranging between  $0.5$  and  $0.9 M_{\odot}$ . Much effort has been spent to extend the equation of state down to the low temperature and high density regime. An analysis of the latest improvement in the physics of white dwarf interiors is presented. We conclude that at the faint end of the cooling sequence ( $\log L/L_{\odot} \sim -5.5$ ) the present overall uncertainty on the age is of the order of 20%, which correspond to about 3 Gyr. We suggest that this uncertainty could be substantially reduced by improving our knowledge of the conductive opacity (especially in the partially degenerate regime) and by fixing the internal stratification of C and O.

*Subject headings:* white dwarfs - age - time scales

## 1. Introduction

In the last few years a growing amount of high-quality data concerning white dwarfs (WDs), both from space as well as from ground based telescopes, have been produced. In particular, the discovery of WD sequences in Globular Clusters (Paresce, De Marchi, & Romaniello 1995, Richer et al. 1997) and the observation of their faint ends in old Open Clusters (Von Hippel, Gilmore, & Jones 1995, Von Hippel & Gilmore 2000) provide new tools for the study of the history of both the halo and the disk of the Milky Way. The possible use of the observed WD sequences as age indicators for a variety of Galactic components is particularly promising. As firstly shown by Mestel (1952), the luminosity of a WD is largely supplied by its thermal energy content, so that the cooling time scale is inversely proportional to a certain power of the luminosity. Thus, comparisons between theoretical estimations of the age-luminosity relation for WDs and the observed cooling sequences may be used to derive stellar ages. On the other side, an accurate comparison between the predictions of the theoretical models with specific observations of WDs could provide a better comprehension of the physical properties of high density matter. In this context the recent development of the asteroseismology applied to WDs allows to check the internal structure of these compact objects (Bradley & Winget 1991, Bradley, Winget, & Wood 1992, Clemens 1993, Metcalfe, Winget, & Charbonneau 2001).

White dwarfs are the final destiny of the evolution of low and intermediate mass stars. The majority of the presently observed WDs are post-Asymptotic Giant Branch stars (AGB). The core of an AGB star is made of ashes of the He-burning, namely a mixture of primary carbon and oxygen, with a minor amount of secondary  $^{22}\text{Ne}$ <sup>1</sup>. During this evolutionary phase the core mass increases, due to the accretion of fresh material processed by the He-burning shell. In the meantime, a huge mass loss erodes the H-rich envelope until it is reduced down to a critical value (see e.g. Castellani, Limongi, & Tornambé 1995), and the star departs from the AGB. About 98 – 99% of the total mass of the resulting WD is the CO core builded up during both the central and shell He-burning phases.  $M_{up}$  is the minimum stellar mass for which a carbon ignition occurs before the onset of the AGB and set the upper mass limit for the progenitors of CO WDs. Current stellar evolution theory predicts that the value of  $M_{up}$  varies between 6.5 and 7.5  $M_{\odot}$ , for metallicity ranging between  $Z=0$  and 0.02 (see Cassisi, Castellani, & Tornambé 1996 and Dominguez et al. 1999 for recent reviews of these calculations). According to a well established theoretical scenario, single stars having mass lower than  $M_{up}$  end their life as CO WDs with masses ranging between about 0.55

---

<sup>1</sup>The original C,N and O nuclei are firstly converted into  $^{14}\text{N}$ , during the H-burning, and, later on during the He-burning, into  $^{22}\text{Ne}$  via the chain  $^{14}\text{N}(\alpha, \gamma)^{18}\text{F}(\beta^+, \gamma)^{18}\text{O}(\alpha, \gamma)^{22}\text{Ne}$ . Thus, the abundance (in number) of  $^{22}\text{Ne}$  in the CO core of a WD roughly correspond to the abundance (in number) of the original CNO.

and  $1.05 M_{\odot}$  (see e.g. Dominguez et al. 1999). The theoretical initial-final mass relation, as derived from stellar evolution models, roughly agrees with the few available measurements of WD masses in nearby Open Clusters (Weidemann & Koester 1983, Weidemann 1987, 2000, Herwig 1997). However, it should be recalled that stellar rotation could induce the formation of more massive CO WD (Dominguez et al. 1996).

Few WDs may have an He-rich core. In principle, stars having initial mass particularly low (namely  $M \leq 0.5 M_{\odot}$ ) never attain temperatures high enough for the He-burning. After the main sequence, they develop a degenerate He core and their final fate should be a low mass He-rich compact remnant. However, owing to the very long evolutionary time scale of these stars (much longer than the Hubble time), we can definitely exclude that the present generation of WDs could include their remnants. Nevertheless, low mass He-rich WDs may result from the deviated evolution of more massive progenitors when, under particular circumstances, a complete envelope removal takes place during the first ascent of the red giant branch. For example, a stripping of the envelope may be caused by a close encounter with another star (Livne & Tuchman 1988) or by Roche lobe overflow in close binary systems (Kippenhahn, Koll, & Weigart 1967, Kippenhahn, Thomas, & Weigart 1968, Iben & Tutukov 1986).

It has been also supposed that massive WDs could be generated by stars having an initial mass slightly larger than  $M_{up}$  (Dominguez, Tornambé, & Isern 1993, Ritossa, Garcia-Berro, & Iben 1996, 1999; Garcia-Berro, Ritossa, & Iben 1997). In this case, in fact, an highly degenerate O-Ne-Mg core is left by the carbon burning. Then, after a rather normal AGB phase, eventually characterized by an important mass loss, these stars could terminate their life as massive ONeMg WDs ( $M \sim 1.2 - 1.3 M_{\odot}$ ).

In this paper, we confine our analysis to the CO WDs having an H-rich envelope, which are the most common type of these compact remnants (the so called DA). Let us note that the physical evolution of the internal structure of a white dwarf appears rather simple when compared to other stellar evolutionary phases. The residual nuclear burnings provide only a negligible contribution to the total luminosity. The highly degenerate core is almost incompressible, so that only the contraction of the most external layers may still contribute to the release of gravitational energy. Only the brightest WDs ( $\log L/L_{\odot} \gtrsim -1.5$ ) suffer a non-negligible energy loss through neutrino production. The cooling time is then determined by the rate of temperature decrease, which depends on the efficiency of the energy transport from the hot core through the thin opaque envelope. A very efficient thermal conduction, due to the highly degenerate electrons, takes place in the whole CO core that rapidly becomes almost isothermal. On the contrary, the more external layers of the WD (i.e. an He-rich mantle and, eventually, an H-rich envelope, where electron are initially only partially or

non degenerate) are efficient insulators and regulate the energy loss rate. Basically, the time scale of the WD evolution is controlled by the heat capacity of the CO core and by the opacity of the external wrap. Thus, the main problem of this studies concerns the accurate evaluation of these two physical ingredients and no sophisticated algorithms for the computation of the stellar structure is, in principle, required. Nonetheless, we believe that the best approach should be that based on a full evolutionary code calculation, which allows a coherent description of both the progenitor and the WD evolution and may account for all the contributions to the energy production and transport.

In this paper we critically re-analyze the influence of the assumed theoretical scheme on the predicted cooling time. In such a way, we try to evaluate the present uncertainty of the cosmo-chronology predictions based on WD models. A rough idea of the present level of uncertainty may be obtained by comparing some recently published theoretical cooling sequences for H-rich atmosphere WD (see figure 1). One may recognize sizeable differences, in particular near the faint end of the cooling sequence. They are likely due to different evaluations of the basic ingredients of the theoretical cooking: the specific heat in the core, the radiative and the conductive opacities, the treatment of the external convection and the like; but they could be also partially attributed to differences in the initial models. We argue that the origin of these uncertainties should be identified before using cooling sequences as cosmic clocks. Owing to the complexity of the matter, our investigation is far from being exhaustive. Many previous works have addressed the question of the reliability of the input physics used in WD models computation. In some case we do not repeat their analysis. For example, we do not address the question of the chemical segregation occurring in the core when the crystallization of the Oxygen component takes place, because this argument has been exhaustively discussed in the recent literature (Segretain et al. 1994, Salaris et al. 1997, Montgomery et al. 1999, Isern et al. 1997, 2000). In some case we extent previous investigations up to the faint end of the cooling sequence, as in the case of the effects of microscopic diffusion. In the following section we illustrate the input physics used to compute the various cooling sequences. In the third section we discuss the uncertainties related to the progenitor evolution that determine the internal stratification of the core and the size of the thin external layers: the He-rich mantel and the H-rich envelope. Section four illustrates the dependence of the cooling time scale on some physical ingredients (EOS, opacity and the like). A final discussion follows.

## 2. Input physics

Our WD models have been obtained by means of a full evolutionary code. In particular we have used the FRANEC in the version described by Chieffi & Straniero (1989). The input physics have been completely revised in order to account for the peculiar conditions developed in WD interiors.

### 2.1. Opacity

We have adopted the radiative opacities of OPAL (Iglesias & Rogers 1996) for high temperature ( $\log T[K] > 4.0$ ) and the Alexander & Ferguson (1994) molecular opacities for the low temperatures ( $\log T[K] \leq 4.0$ ). The conductive opacities have been derived from the work made by Itoh and coworkers (Itoh et al. 1983, Mitake, Ichimaru, & Itoh 1984, Itoh, Hayashi, & Kohyama 1993). Additional models have been obtained by using the Hubbard & Lampe (1969) prescriptions and the table provided by A. Potekhin (see Potekhin et al. 1999). As it is well known (see e.g. Mazzitelli 1994, D’Antona & Mazzitelli 1990), there is a region in the  $T - \rho$  plane not covered by the OPAL radiative opacities and where the electron conductivity is not yet dominant. Thus one has to extrapolate the radiative opacities in order to fill this gap. The problem is alleviated by the use, for the lower temperature, of the Alexander & Ferguson (1994) opacities, which extend at larger densities with respect to the OPAL. Present models have been computed adopting a linear extrapolation of the radiative opacity beyond the upper density provided by OPAL. We have tested the reliability of this choice by changing the extrapolation method. Negligible effects on the cooling sequences have been found.

### 2.2. Nuclear reaction rates and neutrinos

Nuclear reaction are almost extinct during the WD evolution, but they play a relevant role in determine the chemical structure of the model at the beginning of the cooling sequence. We have used the rates tabulated by the NACRE collaboration (Angulo et al. 1999), except for the  $^{12}\text{C}(\alpha, \gamma)^{16}\text{O}$ . During the He-burning this reaction competes with the  $3\alpha$  and regulates the final C/O ratio in the core (Iben 1972). The great influence on the resulting WD evolution has been deeply investigated (D’Antona & Mazzitelli 1990; Salaris et al. 1997). We have used two different rates, namely the one reported by Caughlan et al. (1985) and that of Caughlan & Fowler (1988). Note that the difference between these two compilation may be roughly considered as representative of the present experimental uncertainty level (see

e.g. Buchmann 1996). Nuclear reaction rates are corrected for the weak and intermediate electron screening by using the prescriptions of Graboske et al. 1973 and De Witt, Graboske, & Cooper 1973, and for the strong screening by Itoh, Totsuji, & Ichimaru 1977 and Itoh et al. 1979.

The efficiency of neutrino emission processes are taken from: Haft, Raffelt, & Weiss 1994 (plasma neutrinos), Itoh et al. 1989 (photo and pair neutrinos).

### 2.3. Equation of state

As recognized long ago (Salpeter 1961) Coulomb interactions play a relevant role in WD interior, finally leading to crystallization of the stellar core (Lamb & Van Horn 1975). Thus, a detailed treatment of the thermodynamic behavior of both liquid and solid matter is a necessary physical ingredient to study the evolution of cold WDs. The high pressure experienced in the whole core ensures the complete ionization of carbon and oxygen. Thus, we have updated and extended the EOS for fully ionized matter described by Straniero (1988). In particular, we have revised the treatment of the electrostatic corrections up to the liquid-solid transition and beyond. The free energy in the fluid phase can be written as

$$F_L = F_i^{id} + F_e^{id} + F_i^{ex} + F_e^{ex} + F_{ie}$$

where  $F_i^{id}$  and  $F_e^{id}$  are respectively the contribution of the ideal gas of ions and electrons. To compute these terms, as in Straniero (1988), we have assumed that ions follow the Boltzmann distribution, while electrons are described by Fermi-Dirac integrals, for an arbitrary degree of degeneracy and relativistic state.  $F_i^{ex}$  is the excess of ionic free energy due to ion - ion Coulomb interactions. For this contribution we adopted the analytical expression by Potekhin & Chabrier (2000) that in the region of high ionic coupling parameter ( $\Gamma = (Ze)^2/(ak_B T) \geq 1$ ) fits the accurate results of recent Monte Carlo simulations of one component plasma (De Witt & Slattery 1999), while for  $\Gamma < 1$  it approaches to the Cohen & Murphy (1969) expansion and reproduces the Debye-Huckel limit for vanishing  $\Gamma$  (Landau & Lifshitz 1969). The quantum diffraction correction to ionic free energy has been neglected in the liquid phase.  $F_e^{ex}$  represents the excess electron free energy due to electron - electron interactions. For this term we adopted the non relativistic expression by Tanaka, Mitake, & Ichimaru 1985. We neglected the relativistic  $F_e^{ex}$ . This is a reasonable approximation since at high density, when degenerate electrons become relativistic, the electron coupling parameter  $\Gamma_e \ll 1$ . Finally, for  $F_{ie}$ , that describes the excess due to ion - electron interactions, we adopted the analytical expression given by Potekhin & Chabrier (2000). As it is well known, the contribution of the ion-ion interactions increases with density, eventually

leading to crystallization. According to Potekhin & Chabrier (2000), the liquid-solid phase transition has been assumed at  $\Gamma_c = 175$ . In the solid phase ( $\Gamma \geq \Gamma_c$ ) the free energy can be written as

$$F_S = F_e^{id} + F_i^s + F_e^{ex} + F_{ie} + F_i^{qm}$$

where the electron terms  $F_e^{id}$  and  $F_e^{ex}$  are the same as in the fluid phase. For the free energy of the ionic crystal  $F_i^s$  we used the analytical expression by Farouki & Hamaguchi (1993) obtained by fitting numerical models of molecular dynamic. The contribution of the ion - electron  $F_{ie}$  in the solid phase is from Potekhin & Chabrier (2000). Finally, the term  $F_i^{qm}$  represents the quantum correction to the thermodynamic behavior of the ionic Coulomb crystal. This contribution is very important in late WD evolutionary phases, in fact, as the WD cools down, the crystallized CO core reaches a quantum state (diffraction parameter  $\hbar\Omega_P/(k_B T) > 1$ , where  $\Omega_P$  denotes the ion plasma frequency). When this occurs, the ionic contribution to the specific heat decreases as  $T^3$ , thus depleting the main thermal reservoir of the star: it is called Debye cooling phase. For this term we adopted the analytical expression described by Stolzmann & Blocker (2000), which is based on the free energy of a Coulomb crystal studied by Chabrier, Ashcroft, & De Witt (1992). The various thermodynamic quantities for pure carbon and pure oxygen have been obtained by analytically deriving the corresponding free energy. Finally, an additive volume interpolation is used to calculate the thermodynamic quantities of a CO mixture<sup>2</sup>.

To describe the outer layers of partially ionized helium and hydrogen, we adopted the EOS of Saumon, Chabrier, & Van Horn (1995, SCVH). This EOS requires both high pressure and low pressure extensions. At high pressure ( $P > 10^{19}$  dyn/cm<sup>2</sup>), which is in any case large enough to guarantee a full ionization of H and He, we extended the SCVH EOS following the same procedure described above for the CO core. The match between the two EOS is generally good. At low pressure, we have used a perfect gas (including H, H<sup>+</sup>, H<sub>2</sub>, H<sup>-</sup>, He, He<sup>+</sup> and He<sup>++</sup>) plus radiation. In such a case the classical Saha equation has been used to derive the population of the various species. For each temperature, the precise value of the maximum pressure of the perfect gas (or the minimum of the SCVH) has been varied in order to guarantee a smooth transition between the two EOS.

Tables of this EOS are available on the web.

---

<sup>2</sup>We neglect the contribution of <sup>22</sup>Ne.

## 2.4. Model Atmospheres

In order to fix the external boundary condition of a stellar model, appropriate model atmosphere are needed. In the last decade WD atmosphere theory has significantly improved (Bergeron, Waesemael, & Fontaine 1991; Bergeron, Saumon, & Waesemael 1995; Bergeron, Waesemael, & Beauchamp 1995; Saumon & Jacobson 1999; Bergeron 2000). As it is well known, in the high density/low temperature atmospheres of an old WD the emerging electromagnetic flux significantly departs from the black body spectrum. This is mainly due to the molecular hydrogen recombination and the consequent collision - induced absorption (CIA) by  $H_2 - H_2$  collisions. CIA is the main source of opacity in the infrared and the main cause of increasingly blue color indices for decreasing effective temperature ( $T_e$ ) in cold WDs (Hansen 1998, 1999; Saumon & Jacobson 1999; Bergeron 2000). Detailed model atmospheres are also crucial ingredient to transform the theoretical quantities ( $L$ ,  $T_e$ ) into the observational ones (magnitude, color). In the present computations we have used a solar scaled  $T$ - $\tau$  relation (see Chieffi & Straniero for details) up to the onset of the cooling sequence. Then, namely when  $\log L/L_\odot \sim 0$ , we adopt the model atmospheres of Bergeron, Saumon, & Waesemael (1995), plus a low temperature extension including the effects of the CIA, which has been kindly provided us by P. Bergeron. Since no metals are included in these models, they are consistent with the usual hypothesis of complete sorting of the external layers (see next subsection).

## 2.5. Treatment of convection and other mixing phenomena

Convective boundaries are fixed by using the Schwarzschild criterion. Concerning the progenitor evolution, the extension (in mass) of the convective core during the central He burning have a great influence on the amount of C (and O) in the most internal layers of a WD (Imbriani et al. 2001 and Dominguez et al. 2001). During this phase, we use the algorithm described by Castellani et al. (1985) to take into account the growth of the convective core induced by the conversion of He (low opacity) into C and O (large opacity) and the resulting semiconvection. Breathing pulses, which occur when the central He mass fraction decreases below about 0.1, are usually neglected (but see the discussion in section 3.3). Note that any mechanism that increases the size of the well mixed region during the final part of the He-burning (mechanical overshoot, semiconvection, breathing pulses or rotational induced mixing) leads to a reduction of the resulting amount of C in the central region of the WD (see e.g. Imbriani et al. 2001).

Theoretical studies (Fontaine & Michaud 1979, Iben & MacDonald 1985, 1986, Althaus et al. 2002), supported by observational evidences (see e.g. Bergeron, Ruiz, & Legget 1997),



indicates that, as a consequence of the gravitational settling of heavy elements, DA WDs should have a practically pure H envelope and a pure He mantel. In addition, as suggested by Salaris et al. (1997), the carbon and oxygen profiles left by the He-burning is smoothed by Rayleigh-Taylor instabilities. In order to account for the element diffusion, when  $\log L/L_{\odot} \sim 0$ , we adjust the composition of the envelope and the mantel: all the residual H is putted on the top of a pure He layer. The total mass of H and He is conserved. We also modify the internal C and O profile according the the prescription of Salaris et al. (1997).

Owing to the larger  $\Gamma$ , oxygen crystallization occurs when carbon is still liquid. For a certain time, this occurrence produces an unstable stratification of the liquid phase and, in turn, an efficient mixing (Isern et al. 1997, Salaris et al. 1997). This phenomenon is presently not included in our calculations.

### 3. Pre-WD evolution

First of all one should know the physical and the chemical structure of the star at the beginning of the cooling sequence. Since our investigation regards DA white dwarfs, we need to know the internal stratification of the CO core and the extension (in mass) of both the He and H-rich layers. The formation of the CO core begins during the central He-burning phase and proceeds in the following AGB phase. In principle, a lengthy computation through a series of recursive thermal pulses is required, until the mass loss erodes the envelope and the star becomes a WD (see e.g. Iben & Renzini 1983).

During the thermally pulsing AGB phase, the mass of the CO core is accreted with the ashes of the He-burning shell, while the mass between the two shells is progressively reduced (see e.g. Straniero et al. 1997). Thus, it is very important to determine the duration of the AGB, which is evidently affected by mass loss: the longer the AGB phase, the larger the final mass of the CO core and the smaller the mass of the He-rich mantel. AGB mass loss rate ranges between  $10^{-8}$  and  $10^{-4} M_{\odot}/\text{yr}$ , but it is still unclear how it is related to the changes of the chemical and physical structure occurring in the cool atmospheres of these giants (see Habing 1996). In addition, if the WD progenitor is a low mass star ( $M < 1.5 M_{\odot}$ ), the mass loss during the first ascent to the tip of the red giant branch (RGB) must be also carefully taken into account. The spread in color of the horizontal branch (HB) stars in Globular Clusters is commonly interpreted as an evidence of the different mass loss experienced by similar stars during the RGB phase: bluer HB stars should have a smaller envelope than red HB stars. Since the AGB phase of blue (reduced envelope) HB stars will be significantly shorter than that of a red HB star, the resulting WD will be different. In other words, stars with similar initial mass and chemical composition might produce white dwarfs of different

masses and/or different internal stratification, depending on the mass loss history.

Not only the mass, but also the initial composition of a star determines its evolution and, possibly, its final fate. A detailed descriptions of the internal C and O profiles in WDs generated by stars with mass ranging between 1 and 7  $M_{\odot}$  and metallicity  $0 \leq Z \leq 0.02$  may be found in Dominguez et al. (2001).

This variety of possible progenitor evolutions could frighten the reader. Our scope is to quantify the uncertainty on the cooling time of WD, for different galactic components. Basing on some numerical experiments, we have evaluated the influence of the pre-WD history on the age calibration. Starting from zero age He-burning stellar structures (i.e. an He core surrounded by an H-rich envelope, in which a suitable mixture of Helium and metals is adopted), we have computed the evolutionary sequences up to the WD stage. At the beginning of the cooling phase ( $\log L/L_{\odot} \sim 0$ ) the envelope has been completely sorted in a pure He buffer and a pure H outer envelope mimicking the effect of the very efficient gravitational settling. Table 1 reports the initial parameters of the models and the properties of the resulting white dwarfs, namely: identification label of the model, initial mass ( $M_{ZAHB}$ ), metallicity ( $Z$ ), initial He-core mass ( $M_{He}$ ), final mass ( $M_{WD}$ ), final amount of He ( $\Delta M_{He}$ ), final amount of H ( $\Delta M_H$ ), central carbon mass fraction ( $X_C$ ), mass of the homogeneous central region ( $Q=M_{flat}/M_{WD}$ , see below for a definition of this parameter), WD age when  $\log L/L_{\odot}=-5.5$ .

### 3.1. Comparison between different evolutionary tracks leading to the same WD mass

Let us firstly discuss models B, B1, B2. The total mass has been maintained constant ( $M=0.6 M_{\odot}$ ) during the whole evolution for both case B and B1. They differ for the initial mass of the H-rich envelope, namely:  $10^{-3}$  and  $2 \cdot 10^{-2} M_{\odot}$  respectively for B and B1. The third case (B2) has been computed starting from a larger mass ( $M=0.64 M_{\odot}$ ) and imposing a constant mass loss ( $3 \cdot 10^{-8} M_{\odot}/yr$ ) since the onset of the thermally pulsing phase. In this case, the initial He-core mass is in agreement with recent evolutionary computation of H-burning models of low mass stars (see e.g. Straniero, Chieffi, & Limongi 1997). Note that the initial total mass has been chosen to obtain a final (WD) mass similar to the (constant) one of case B and B1. A low metallicity ( $Z=10^{-4}$ ), adequate for old halo WD progenitors, has been chosen for all these three models. Figure 2 illustrates the evolutionary tracks in the HR diagram. The central He-burning phase is similar in the three cases. At the central He exhaustion, model B1 evolves toward the red part of the HR diagram and develops the typical double shell structure of an AGB star. When the faster He-burning shell get closer

to the H-burning one, it dies down and the star enters in the thermally pulsing phase (for a more detailed description see e.g. Iben & Renzini 1983). After two major thermal pulses, the envelope mass is reduced down to about  $0.001 M_{\odot}$ ; then, the star leaves the AGB. During the post-AGB, a further (last) thermal pulse takes place; the star re-expand and comes back to the asymptotic giant branch. Finally, after a second horizontal crossing of the HR diagram, both shells definitely die down and the model settles on the WD cooling sequence.

Owing to the very small envelope mass, after the central He exhaustion, model B remains in the blue side of the HR diagram, so skipping the classical AGB phase. When the outgoing He shell approaches the H-rich layer it dies down. Note that the H-burning shell has been practically inactive up to this moment. The following contraction of the star induces some irregular and short H-ignitions. Finally this model attains its cooling sequence.

In model B2 the duration of the AGB and the final WD mass are mainly determined by the assumed mass loss rate, which is, in any case, quite typical for faint TP-AGB stars. This models experience 8 thermal pulses; then, the envelope is reduced down to a certain critical value and the model moves toward the blue side of the HR diagram (see figure 2). Note that the mass loss has been stopped when the effective temperature becomes larger than 7000 K. At variance with case B1, no more thermal pulses are found in the post-AGB phase.

The resulting profiles of carbon and oxygen in the core of the three final WD models are shown in figure 3. The most internal region is produced during the central He-burning and its flatness is a consequence of the convective mixing occurring in the stellar core. As noted by Salaris et al. (1997), the region immediately outside the flat profile left by the central convection presents a positive gradient of mean molecular weight. The consequent Rayleigh-Taylor instability induces a mixing and a further little reduction of the central carbon. In column 8 and 9 of table 1 we have reported the central C mass fraction and the mass of the homogeneous central region (in unit of the total WD mass) as they should result after the action of this Rayleigh-Taylor instability ( $Q=M_{flat}/M_{WD}$ ). The growing C profile in the more external layer is produced during the AGB, when the He-burning shell advances in mass toward the stellar surface. The carbon peak at the external border of the CO core reflects the incomplete He-burning left by the last thermal pulse. The three chemical structures are rather similar. In particular the amount of carbon (oxygen) in the center of the WD and the extension of the inner flat region are practically the same. The most relevant differences is the size (in mass) of the He-rich mantel (see column 6 in table 1). In model B1 the thickness of the mantel is about half of that found in case B. This is the memory of the last thermal pulse experienced by model B1 in the post-AGB phase, when the H-burning shell was almost extinct.

The amount of hydrogen left in the envelope of the WD is practically the same in

the three models. This confirms the fact, already demonstrated in many papers, that for each metallicity and core mass, it exist a maximum mass of the H-rich envelope for a WD (Iben 1982, Fujimoto 1982a,b, Castellani, Degl’Innocenti, & Romaniello 1994, Piersanti et al. 2000). When the H mass exceeds such a limit, the H-burning is efficiently activated at the base of the envelope. It drives the expansion of the envelope leading to the formation of a giant star rather than to a white dwarf.

The cooling sequence obtained starting from the three pre-WD models illustrated in this subsection are shown in figure 4. They are very similar, with a little difference (less than 0.5 Gyr) at the faint end. In particular, the cooling of model B1 is a bit faster because the smaller He mantel. Note that these three models reach the WD stage through a very different path and they may be considered as representative of the possible changes occurring during the progenitor evolution. In summary, the knowledge of the cooling time scale at the faint end of the WD sequence (namely at  $\log L/L_{\odot}=-5.5$ ) is limited by a 3-4% error as a consequence of the uncertainty on the leading parameters characterizing the pre-WD history.

### 3.2. Influence of the initial metallicity

In many recent studies of cosmochronology (Salaris et al. 1997, Richer et al. 2000) WD models based on progenitors having solar chemical composition have been used. This is certainly adequate to study the age of the disk and its components (Open Clusters). However, when the main goal are the oldest component of our Galaxy, halo or Globular Cluster stars, low metallicity models are more appropriate. In this subsection we would try to evaluate the influence on the cooling sequence of the progenitor chemical composition. For this reason we have computed an additional model producing a WD having  $M=0.6 M_{\odot}$ , but with a solar metallicity, namely  $Z=0.02$ .

The properties of this model are reported in the fourth row of table 1 (model B3). A comparison with model B ( $Z=0.0001$ ) reveals only small differences. As already discussed by Dominguez et al. (2001), the central carbon abundance is slightly lower at large metallicity; they found a maximum 10% variation when the metallicity is varied between 0.0001 and 0.02. Note that the extension of the innermost homogeneous region decreases by increasing the metallicity (see the values reported in column 9 of table 1). As expected, since the H-burning is more efficient at large metallicity (because the larger amount of CNO), the mass of the H-rich envelope is significantly reduced when the star attains the cooling sequence. In spite of this difference, at the faint end model B3 is only 2% younger than model B. The cooling sequences obtained for the two metallicities are compared in figure 5.

### 3.3. Internal Stratification: $^{12}\text{C}(\alpha, \gamma)^{16}\text{O}$ and turbulent convection

The amounts of carbon and oxygen left in the core of a WD have a great influence on its cooling rate (D’Antona & Mazzitelli 1990, Salaris et al. 1997) and plays an important role in determining the observable outcome of a type Ia supernova (Dominguez et al. 2001). The chemistry of a WD is determined by the competition of the two major nuclear reactions powering the He burning, namely the  $3\alpha$  (the carbon producer) and  $^{12}\text{C}(\alpha, \gamma)^{16}\text{O}$  (the carbon destroyer). As deeply discussed by Imbriani et al. (2001), the final C/O not only depends on the rate of these two reactions, but it is significantly influenced by the efficiency of the convective mixing operating near the center of an He burning star. The pre-WD models discussed so far, has been obtained by neglecting any source of extra-mixing, like mechanical overshoot, possibly occurring at the external edge of the convective core. We have also suppressed the so called breathing pulses, which take place when the central mass fraction of He is reduced down to  $\sim 0.1$  (see Castellani et al. 1985 and references therein). As shown by Imbriani et al. (2001), the amount of carbon left in the center is almost insensitive to the occurrence of the convective overshoot, but it is strongly influenced by any additional mixing occurring in the final part of the He-burning, when the carbon previously accumulated by the  $3\alpha$  is efficiently converted into oxygen via the  $^{12}\text{C}(\alpha, \gamma)^{16}\text{O}$  reaction. This is exactly the job done by breathing pulses (BPs). In this subsection we study the combined effects of a change of the  $^{12}\text{C}(\alpha, \gamma)^{16}\text{O}$  rate and the inclusion of BPs. Models B to B3 have been obtained by using a high rate for the  $^{12}\text{C}(\alpha, \gamma)^{16}\text{O}$  reaction (namely, the one reported by Caughlan et al. 1985, hereinafter C85). As it is well known, the adoption of a low rate leads to a significantly larger central abundance of carbon. Model B-low has been obtained by adopting the rate reported by Caughlan & Fowler (1988, hereinafter CF88), which is about 0.4 times the rate of C85 at the relevant temperatures (around  $2 \times 10^8$  K). Recent experimental determinations of this rate (Buchmann 1996 and 1997, Kunz et al. 2001, 2002) seem to confirm that the actual value should be intermediate between CF88 and C85. Then, we have also repeated these two calculations by including the effect of the breathing pulses (model B-BP and B-low-BP). The internal chemical profiles of models B-low and B-low-BP are compared in figure 6, while the influence on the cooling sequence is illustrated in figure 7. In synthesis, the whole uncertainty (convection plus nuclear reaction rate) due to the He-burning phase induces a 9% uncertainty in the estimated cooling time at the faint end of the WD sequence (see the values reported in the last column of table 1). It is worth noting that this is only a lower limit of the uncertainty caused by the possible variation of the internal composition. In fact, as discussed by Isern et al. (1997) and Montgomery et al. (1999), the delay of the cooling due to the chemical segregation upon crystallization is larger when  $X_C \sim X_O$ . Therefore, the occurrence of this phenomenon should hampers the differences between case B-low and case B-BP. A more quantitative estimation may be deduced from the results reported in

table 2 of Montgomery et al.. Note that our B-low model have an internal stratification that roughly correspond to their 50:50 case, while our model B have a composition profile similar to the one of Salaris et al. (1997). Then, according to Montgomery et al., element segregation should increase the age difference between B-low and B-BP of at least 0.6 Gyr, thus bringing the whole uncertainty on the age at the faint end of the cooling sequence up to 13-14%.

### 3.4. The thickness of the H-rich envelope

We have already discussed the existence of a maximum value for the mass of the H-rich envelope of a WD. However, the actual amount of H at the top of a WD could be substantially lower. In fact, stellar wind may continue during the post-AGB phase so that the H-rich envelope could be strongly reduced and even completely lost. It is well known that in an important fraction (about 10-20 %) of the whole WD population the H-rich envelope is practically absent (DB-WDs). The minimum detectable amount of H is very low (about  $10^{-10} M_{\odot}$ ). The post-AGB mass loss is the easiest explanation of the lack of H in the atmosphere of the DB WD. An alternative possibility was advanced by Iben & Renzini (1983). They suggested that the progenitors of the DB could have suffered a last thermal pulse during the post-AGB, when the H-burning shell is almost extinguished. In this condition, the convective shell generated by the thermal pulse could completely mix the He and the H-rich layers. Then, the H dredged down at high temperature is rapidly consumed. We recall that a similar post-AGB thermal pulse has been encountered in our model B1, but no evidence of a deep H mixing has been found (in this particular case).

D’Antona & Mazzitelli (1989) and Tassoul et al. (1990) have investigated the WD properties by changing the amount of H in the envelope. However, due to the lack of reliable opacity and EOS, they didn’t extent the computation down to the faint end of the cooling sequence. Then, we have computed two additional cooling sequences by artificially reducing the H-rich layer of model B, namely:  $\Delta M_H = 3.12 \cdot 10^{-5}$  and  $2.32 \cdot 10^{-6} M_{\odot}$  for model B-LH and B-VLH, respectively (row 5 and 6 of table 1). The comparison between these two models and model B is shown in figure 8. As expected, the cooling is faster in models with a smaller envelope. The age reduction at  $\log L/L_{\odot} = -5.5$  would be as large as 1 Gyr if the residual mass of the H-rich envelope was of the order of  $10^{-10} M_{\odot}$ .

## 4. The physics of WD interior

In this section we address the uncertainty caused by some input physics directly affecting the WD evolution.

### 4.1. Conductive Opacities

Degenerate electrons dominates the heat conduction in white dwarf interiors. Two different tabulations of the thermal conductivity by electrons are commonly used in the computation of WD models, namely: the one presented by Hubbard & Lampe (1969, hereinafter HL69) and those by Itoh and coworkers (Itoh et al. 1983, Mitake et al. 1984, Itoh et al. 1993, hereinafter I93). HL69 considered partially degenerate electrons scattered by ions. They also included the effect of the electron-electron interaction, which is negligible in extreme degeneracy regime (due to the Pauli exclusion principle), but becomes important if degeneracy is not strong, as in the external region of a WD. The main limitation of this calculation is due to the assumption of non-relativistic electrons. In practice, the Hubbard and Lampe conductive opacities are only adequate for densities lower than  $10^6$  g/cm<sup>3</sup>. Actually, a stronger limitation of this calculation is often ignored. In fact, in order to smooth out the discontinuity in the conductive opacity occurring at the liquid/solid phase transition, the conductive opacities were artificially and progressively increased for  $\Gamma \geq 10$ . Let us recall that at the end of the Sixties it was believed that the phase transition from liquid to solid would occur for rather low values of the Coulomb coupling parameter ( $50 < \Gamma < 100$ ). This explains the choice of a particularly low  $\Gamma$  to manage the discontinuity occurring at the phase transition. Nevertheless, the most recent studies find that the crystallization begins at  $\Gamma \sim 170 - 180$  (we adopt 175), in any case well above  $\Gamma = 10$ . The work made by Itoh and coworkers is a substantial improvement of the calculation of electron conduction. They treat inter-ionic correlations and electron-ion interactions by means of an improved theory, based on one-component Monte Carlo calculation. However, since they assume fully degenerate electrons, their opacities are only accurate for large value of the degeneracy parameter. At lower density (or at larger temperature), I93 probably underestimate the effects of the electron-electron interactions.

In figure 9 we illustrate the situation in the case of the core of our reference model (B). The empty area in the left panel shows the allowed region in the case of HL69, while the right panel refers to I93. The two (almost vertical) series of arrows shows the evolution of the physical conditions at the center and at the external boundary of the core. This figure demonstrate that HL69 is not adequate to describe the heat conduction in the major part of the WD structure, even if the density is somewhat lower than the relativistic limit. On

the contrary the condition of extreme degeneracy is well satisfied and the I93 assumption seems appropriated for the whole CO core. Concerning the more external layers, figure 10 illustrate the case for the He-rich mantel. As in figure 9, the left and the right panel show the region of validity for HL69 and I93, respectively. The two series of arrows marks the boundaries of the mantel. HL69 should be preferred in the first part of the cooling sequence, since electrons may be partially degenerate while  $\Gamma$  is generally rather small. The situations change toward the faint end of the cooling sequence, during which the I93 should be more appropriate. Note that there exist a thin region in the  $T$ - $\rho$  plane in which both calculation are, in principle, valid. It happens, for example in the case of an He-rich mixture, for  $\theta \sim 0.1$ . The thick line in figure 10 marks this condition. However, a comparison along the  $\theta=0.1$  line shows that the HL69 opacities are generally larger (20-40 %) than the I93 ones. Such a mismatch reveals a more profound difference between the two calculations, which cannot be easily understood.

In figure 11 we report the cooling sequences obtained by using the HL69 and I93 (case B-HL69 and case B, respectively). In the former case, we have generated the conductive opacities by means of the original code provided by Hubbard. As expected, the lower cooling rate obtained with Hubbard & Lampe reflects the larger value of the conductive opacities. Note that the major discrepancies between the two cooling sequences occurs at about  $\log(L/L_{\odot})=-4$ , exactly when electron conduction becomes the dominant mechanism of energy transportation at the base of the convective envelope. As it is well known (see e.g. Tassoul et al. 1990), this occurrence produces a temporary reduction of the cooling rate. Since many authors use a combination of the HL69 and I93, in figure 11 we have also reported an additional model obtained by using I93 for  $\theta < 0.1$  and HL69 elsewhere (case B-comb). This test shows that the discrepancy mainly concerns the conductive opacity in the weakly-degenerate regime. In conclusion, no ones of the prescriptions widely adopted in the computation of models of WDs appear adequate to describe the whole structure of these cool stars. Unfortunately, the substantial disagreement, at temperature and density for which both computations should be correct, suggests extreme caution in using combined tables. Since the differences of these two theoretical prescriptions imply a 17% variation in the estimated WD age (at the faint end of the cooling sequence, see the last column in table 1), we conclude that the calculation of the conductive opacities (especially in partially degenerate regime) deserves much attention in view of a reliable calibration of the WD cooling time. In this context a recent paper by Potekhin et al. (1999, see also Potekhin 1999) address this problem, extending the computation of electron conductivity to the weakly-degenerate regime. Other improvements, as, in particular, refined ion structure factors and multi-phonon scattering, have been included. The conductive opacity obtained by Potekhin and coworkers are intermediate between those of HL69 and I93. Nevertheless, as shown in



figure 11, the resulting cooling sequence does not substantially differs from the one obtained by using the I93. On the contrary, the cooling time is significantly smaller than those obtained in the model B-HL69 and B-comb. Some properties of the model obtained by means of the electron conductivity calculated by Potekhin et al. (1999) are reported in table 1 (model B-Pot).

#### 4.2. EOS: ion-electron interaction

Chabrier et al. 2000 compare WD cooling sequences obtained by changing the prescriptions for the contribution of the ion-electron interactions to the free energy. In particular they found a significant decrease of the cooling time (about 10%) when the prescription of Potekhin & Chabrier (2000) are used in the solid phase instead of the result given by Yakovlev & Shalybkov (1989). As pointed out by Potekhin and Chabrier, the ion-electron interactions are generally negligible, except in the solid state at very high density. For carbon the ion-electron contribution to the heat capacity becomes very important at  $T=10^5$  K and  $\rho > 10^6$  g cm<sup>-3</sup> but at  $T=10^6$  K,  $\rho$  must be larger than  $10^8$  g cm<sup>-3</sup>, a density never attained in CO white dwarfs (see figure 8 of Potekhin & Chabrier). We have investigated the overall effect of this contribution to the heat capacity by computing an additional model (model B-noie) by fully neglecting the ion-electron interactions. We recall that our "standard" computation are based on the Potekhin & Chabrier prescription. The result is shown in figure 12 (see also table 1). This test clearly demonstrates that the contribution of the ion-electron interaction derived by Potekhin & Chabrier produces a negligible effect on the cooling of CO white dwarfs.

#### 4.3. External Stratification: microscopic diffusion

Many studies have shown that the time-scale of diffusion is short enough to sort the external layers of a WD, thus explaining the observed mono-elemental feature of WD spectra (Fontaine & Michaud 1979, Muchmore 1984, Paquette et al. 1986). Many authors have discussed the effects of diffusion on the WD structure and evolution (see in particular Iben & MacDonald 1985 and 1986, Althaus et al. 2002). All the models presented here have been obtained by assuming a complete sorting of the H and He layers at the beginning of the cooling sequence ( $\log L/L_{\odot} \sim 0$ ). Since we are mainly interested in quantify the overall variation of the cooling time, we have computed a new model in which the chemical stratification of both the envelope and the mantel is the one modeled by the nuclear burning and, eventually, by convection (model B-nodif). We note that the adopted model atmospheres does

not include the effect of metals. Since the assumed metallicity is quite low ( $Z=0.0001$ ), the consequent inconsistency should not dramatically affect our result. The comparison between the properties of this model and those of the *standard* one (model B) is illustrated in figure 13 and in table 1. In the standard case, the larger radiative opacity of the pure H induces the formation of a deeper convective envelope. As a consequence, the slow cooling phase, which takes place when the internal border of the convective layer reaches the region dominated by electron conduction, is anticipated. In conclusion, at the faint end of the cooling sequence, the model in which the effect of microscopic diffusion are neglected is a 11% younger than the standard model. Note that this is the younger model we found.

## 5. Cooling time and WD mass

As it is well known the cooling time depends, among the other things, on the WD mass. Figure 14 shows models in the mass range  $0.5 - 0.9 M_{\odot}$  computed under the same prescriptions adopted for the case B. In table 2 we have summarized the properties of these models. Isochrones and luminosity functions based on these models are available on the web.

## 6. Summary and Conclusions

In the last decade cosmochronology based on WDs has become a promising tool of scientific inquiry thanks to both the availability of a large amount of high quality data for cool and faint WDs and the improvement of the understanding of the high density plasma physics. However, as demonstrated by the rather large discrepancies among the recently published theoretical cooling sequences, a firm calibration of the age-luminosity relation is still not available.

We have analyzed some of the main sources of uncertainty affecting the theoretical cooling time. Physical and chemical parameters characterizing the white dwarfs and the progenitors evolutions have been revised.

Concerning progenitors, we found that the larger uncertainty is due to the combined action of convective mixing a nuclear reactions operating during the central He-burning phase. Both these processes are largely affected by theoretical and experimental uncertainties. They determine the amount of C (and O) left in the core of the WD and, in turn, have a great influence on the predicted cooling rate. A conservative analysis allow us to conclude that the overall impact of the uncertainties due to the progenitors evolution on the estimated WD ages at  $\log L/L_{\odot} = -5.5$  is of the order of 2 Gyr. We hope that this uncertainty will be

significantly reduced in the next future thanks to the renewed effort of nuclear physicists in measuring the  $^{12}\text{C}(\alpha, \gamma)^{16}\text{O}$  reaction rate at low energy (see Gialanella et al. 2001 and Kunz et al. 2001).

Concerning WD physics we emphasize the relevance of a reliable description of the electron conductivity which is the main mechanism of energy transport in WD interiors. Actually, a consistent part of the large discrepancies found in the comparisons of published cooling sequences may be due to the adopted conductive opacity. The old Hubbard and Lampe (1969) conductive opacity are probably overestimated, even in the weakly degenerate regime. The latest computations by Itoh and coworkers and Potekhin et al. (1999) imply a substantial reduction of the age. At  $\log L/L_{\odot} = -5.5$ , we obtain models  $\sim 2.5$  Gyr younger than that obtained with HL69.

Let us conclude by noting that most of the uncertainties discussed in this paper mainly affect old WDs, but have negligible influence on the age estimated for young WDs, whose luminosity is larger than  $10^{-4} L_{\odot}$ . This implies that the presently available theoretical scenario may be safely used to estimate the age of young stellar systems as, for example, the intermediate age Open Clusters ( $t < 3$  Gyr).

#### **Acknowledgments:**

We wish to thank P. Bergeron for kindly providing us the models atmosphere and S. Degl’Innocenti, Luciano Piersanti and Jordy Isern for the many helpful comments. We thank also S. Shore for the careful reading of the manuscript and the several useful discussions. We are deeply indebted to V. Castellani for continuous encouragements and for a critical review of the manuscript. This work has been supported by the MIUR Italian grant Cofin2000.

#### **REFERENCES**

- Alexander D.R., & Ferguson J.W. 1994, ApJ, 437, 879
- Althaus, L.G., Serenelli, A.M., Corsico, A.H., & Benvenuto, O.G. 2002, MNRAS, 330, 685
- Angulo, C. et al. 1999, Nucl. Phys. A, 656, 3
- Benvenuto, O.G., & Althaus, L.G. 1999, MNRAS, 303, 30
- Bergeron, P. 2000, private communication
- Bergeron, P., Ruiz, M.T., & Leggett, S.K. 1997, ApJS, 108, 339
- Bergeron, P., Saumon, D., & Wesemael, F. 1995, ApJ, 443, 764

- Bergeron, P., Wesemael, F., & Beauchamp, A. 1995, *PASP*, 107, 1047
- Bergeron, P., Wesemael, F., & Fontaine, G. 1991, *ApJ*, 367, 253
- Bradley, P.A., & Winget, D.E. 1991, *ApJS*, 75, 463
- Bradley, P.A., Winget, D.E., & Wood, M.A. 1992, *ApJ*, 391, L33
- Buchmann, L. 1996, *ApJ*, 468L, 127
- Buchmann, L. 1997, *ApJ*, 479L, 153
- Cassisi, S., Castellani, V., & Tornambé, A. 1996, *ApJ*, 459, 298
- Castellani, M., Limongi, M., & Tornambé, A. 1995, *ApJ*, 450, 275
- Castellani, V., Chieffi, A., Tornambé, A., & Pulone, L. 1985, *ApJ*, 296, 204
- Castellani, V., Degl’Innocenti, S., & Romaniello, M. 1994, *ApJ*, 423, 266
- Caughlan, G.R., & Fowler, W.A. 1988, *Atomic Data Nucl. Data Tables*, 40, 283
- Caughlan, G.R., Fowler, W.A., Harris, M.J., & Zimmermann, B.A. 1985, *Atomic Data Nucl. Data Tables*, 32, 197
- Chabrier, G., Ashcroft, N.W., & De Witt, H.E. 1992, *Nat.*, 360, 48
- Chabrier, G., Brassard, P., Fontaine, G., & Saumon, D. 2000, *ApJ*, 543, 216
- Chieffi A., & Straniero O. 1989, *ApJ*, 71, 47
- Clemens, J.C. 1993, *Baltic. Astron.*, 2, 407
- Cohen, E.G.D., & Murphy, T.J. 1969, *Phys. Fluids*, 12, 1404
- D’Antona, F., & Mazzitelli, I. 1989, *ApJ*, 347, 934
- D’Antona, F., & Mazzitelli, I. 1990, *ARA&A*, 28, 139
- De Witt, H.E., Graboske, H.C., & Cooper, M.S. 1973, *ApJ*, 181, 439
- De Witt, H., & Slattery, W. 1999, *Contrib. Plasma Phys.*, 39, 97
- Dominguez, I., Chieffi, A., Limongi, M., & Straniero, O. 1999, *ApJ*, 524, 226
- Dominguez, I., Höflich, P., & Straniero, O. 2001, *ApJ*, 557, 279

- Dominguez, I., Straniero, O., Tornambé, A., & Isern, J. 1996, *ApJ*, 472, 783
- Dominguez, I., Tornambé, A., & Isern, J. 1993, *ApJ*, 419, 268
- Farouki, R.T., & Hamaguchi, S. 1993, *Phys. Rev. E.*, 47, 4330
- Fontaine, G., & Michaud, G. 1979, *ApJ*, 231, 826
- Fujimoto, M.Y. 1982a, *ApJ*, 257, 767
- Fujimoto, M.Y. 1982b, *ApJ*, 257, 752
- Garcia-Berro, E., Ritossa, C., & Iben, I.Jr. 1997, *ApJ*, 485, 765
- Gialanella et al. 2001, *Eur. Phys. J.A.*, 11, 357
- Graboske, H., De Witt, H., Grossman, A., & Cooper M. 1973, *ApJ*, 181, 457
- Haft, M., Raffelt, G., & Weiss A. 1994, *ApJ*, 425, 222
- Habing, H.J. 1996, *A&A Rev*, 7, 97
- Hansen, B.M. 1998, *Nat.*, 394, 860
- Hansen, B.M. 1999, *ApJ*, 520, 680
- Herwig, F. 1997, in *Proceedings of the 10th European Workshop on White Dwarfs*, held in Blanes, Spain, 17-21 June 1996. Ed. J. Isern, M. Hernanz, and E. Gracia-Berro. Publisher: Dordrecht: Kluwer Academic Publishers, 1997
- Hubbard, W.B., & Lampe, M. 1969, *ApJS*, 18, 297
- Iben, I.J., 1972, *ApJ*, 178, 433
- Iben, Jr.I. 1982, *ApJ*, 259, 244
- Iben, Jr.I., & MacDonald, J. 1985, *ApJ*, 296, 540
- Iben, Jr.I., & MacDonald, J. 1986, *ApJ*, 301, 164
- Iben, Jr.I., & Renzini, A. 1983, *ARA&A*, 21, 271
- Iben, Jr.I., & Tutukov, A.V. 1986, *ApJ*, 311, 742
- Iglesias, A., & Rogers, F.J. 1996, *ApJ*, 464, 943

- Imbriani, G., Limongi, M., Gialanella, L., Terrasi, F., Straniero, O., & Chieffi, A. 2001, *ApJ*, 558, 903
- Isern, J., Garcia-Berro, E., Hernanz, M., & Chabrier, G. 2000, *ApJ*, 528, 397
- Isern, J., Mochkovitch, R., Garcia-Berro, E., & Hernanz, M. 1997, *ApJ*, 485, 308
- Itoh, N., Adachi, T., Nakagawa, M., Kohyama, Y., & Munakata, H. 1989, *ApJ*, 339, 354
- Itoh N., Hayashi, H., & Kohyama, Y. 1993, *ApJ*, 418, 405
- Itoh N., Mitake S., Iyetomi H., & Ichimaru S., 1983, *ApJ*, 273, 774
- Itoh, N., Totsuji, H., & Ichimaru, S. 1977, *ApJ*, 218, 477
- Itoh, N., Totsuji, H., Ichimaru, S., & De Witt, H. 1979, *ApJ*, 234, 1079
- Kippenhahn, R., Kohl, K., & Weigert, A. 1967, *Zeitschrift fur Astrophysik*, 66, 58
- Kippenhahn, R., Thomas, H.C., & Weigert, A. 1968, *Zeitschrift fur Astrophysik*, 69, 265
- Kunz R., Jaeger F.M., Mayer A., & Hammer J.W. 2001, *Phys. Rev. Lett.*, 86, 3244
- Kunz R., Jaeger F.M., Mayer A., Hammer J.W. , Staudt, G., Harissopulos, S., & Paradellis, T. 2002, *ApJ*, 567, 643
- Lamb, D. Q., & Van Horn, H. M. 1975, *ApJ*, 200, 306
- Landau, L.D., & Lifshitz, E.M. 1969, "Statistical Physics", Pergamon, Oxford
- Livne, E., & Tuchman, Y. 1988, *ApJ*, 332, 271
- Mazzitelli, I. 1994, "The equation of state in astrophysics", Proceedings of IAU Colloquium No. 147, Saint-Malo, France, 14-18 June 1993, Cambridge: Cambridge University Press, 1994, ed. G. Chabrier and E. Schatzman, p.144
- Mestel, L. 1952, *MNRAS*, 112, 583
- Metcalfe, T.S., Winget, D.E., & Charbonneau, P. 2001, *ApJ*, 557, 1021
- Mitake, S., Ichimaru, S., & Itoh, N. 1984, *ApJ*, 277, 375
- Montgomery, M.H., Klumpe, E.W., Winget, D. E., & Wood, M.A. 1999, *ApJ*, 525, 482
- Muchmore, D. 1984, *ApJ*, 278, 769

- Paquette, C., Pelletier, C., Fontaine, G., & Michaud, G. 1986, *ApJS*, 61, 197
- Paresce, F., De Marchi, G., & Romaniello, M. 1995, *ApJ*, 440, 216
- Piersanti, L., Cassisi, S., Iben, I.Jr., & Tornambé, A. 2000, *ApJ*, 535, 932
- Potekhin, A.Y. 1999, *A&A*, 351, 787
- Potekhin, A.Y., Baiko, D.A., Haensel, P., & Yakovlev, D.G. 1999, *A&A*, 346, 345
- Potekhin, A.Y., & Chabrier, G. 2000, *Phys. Rev. E.*, 62, 8554
- Richer, H.B. et al. 1997, *ApJ*, 484, 741
- Richer, H.B. et al. 2000, *ApJ*, 529, 318
- Ritossa, C., Garcia-Berro, E., & Iben, Jr.I 1996, *ApJ*, 460, 489
- Ritossa, C., Garcia-Berro, E., & Iben, Jr.I 1999, *ApJ*, 515, 381
- Salaris, M., Dominguez, I., Garcia-Berro, E., Hernanz, M., Isern, J., & Mochkovitch, R. 1997, *ApJ*, 486, 413
- Salaris, M., Garcia-Berro, E., Hernanz, M., Isern, J., & Saumon, D. 2000, *ApJ*, 544, 1036
- Salpeter, E.E. 1961, *ApJ*, 134, 669
- Saumon, D., Chabrier, G., & Van Horn, H.M. 1995, *ApJS*, 99, 713
- Saumon, D., & Jacobson, S.B. 1999, *ApJ*, 511, L107
- Segretain, L., Chabrier, G., Hernanz, M., Garcia-Berro, E., Isern, J., & Mochkovitch, R. 1994, *ApJ*, 434, 641
- Stolzmann, W., & Blocker, T. 2000, *A&A*, 361, 115
- Straniero, O. 1988, *A&A*, 76, 157
- Straniero, O., Chieffi, A., & Limongi, M. 1997, *ApJ*, 490, 425
- Straniero, O., Chieffi, A., Limongi, M., Busso, M., Gallino, R., & Arlandini, C. 1997, *ApJ*, 478, 332
- Tanaka, S., Mitake, S., & Ichimaru, S. 1985, *Phys. Rev. A*, 32, 1896
- Tassoul, M., Fontaine, G., & Winget, D.E. 1990, *ApJS*, 72, 335

- Von Hippel, T., Gilmore, G., & Jones, D.H.P. 1995, MNRAS, 273L, 39
- Von Hippel, T., & Gilmore, G. 2000, AJ, 120, 1384
- Weidemann, V. 1987, A&A, 188, 74
- Weidemann, V. 2000, A&A, 363, 647
- Weidemann, V., & Koester, D. 1983, A&A, 121, 77
- Wood, M.A. 1995, in “White Dwarfs”, Springer Verlag, ed: D. Koester & K. Werner, 41
- Yakovlev, D., & Shalybkov, D. 1989, Astron. Space Phys. Rev., 7, 311



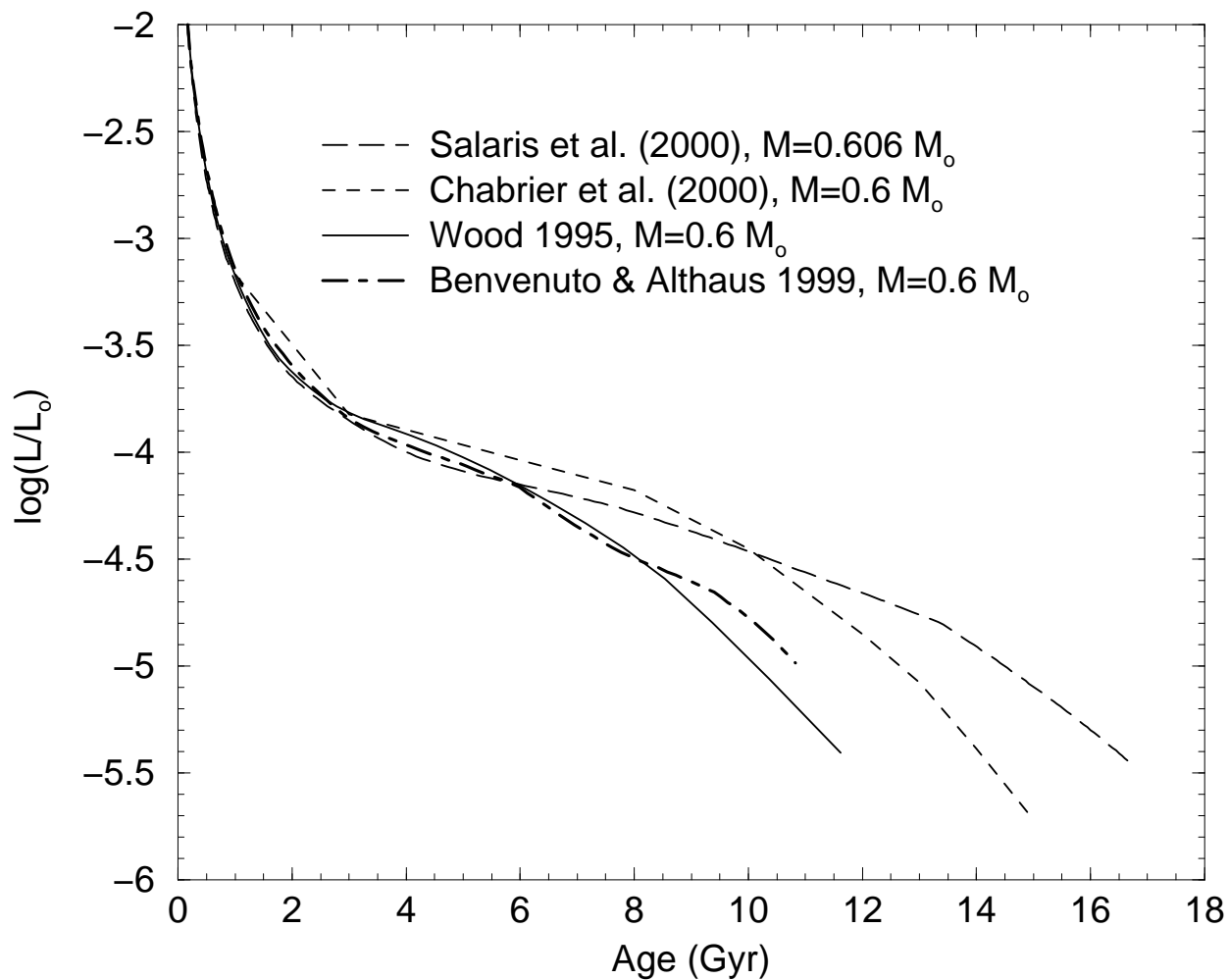


Fig. 1.— Comparison between some of the most recent theoretical cooling sequences for a DA WD of  $M=0.6 M_{\odot}$ : Salaris et al. 2000 (long dashed line), Chabrier et al. 2000 (dashed line), Wood 1995 (solid line), Benvenuto & Althaus 1999 (dot-dashed line). All these sequences, except the one of Chabrier et al 2000, have been computed without including the effect of the chemical segregation occurring upon crystallization and by using a full evolutionary code. The Chabrier et al. sequence has been derived from static WD models and include chemical segregation.

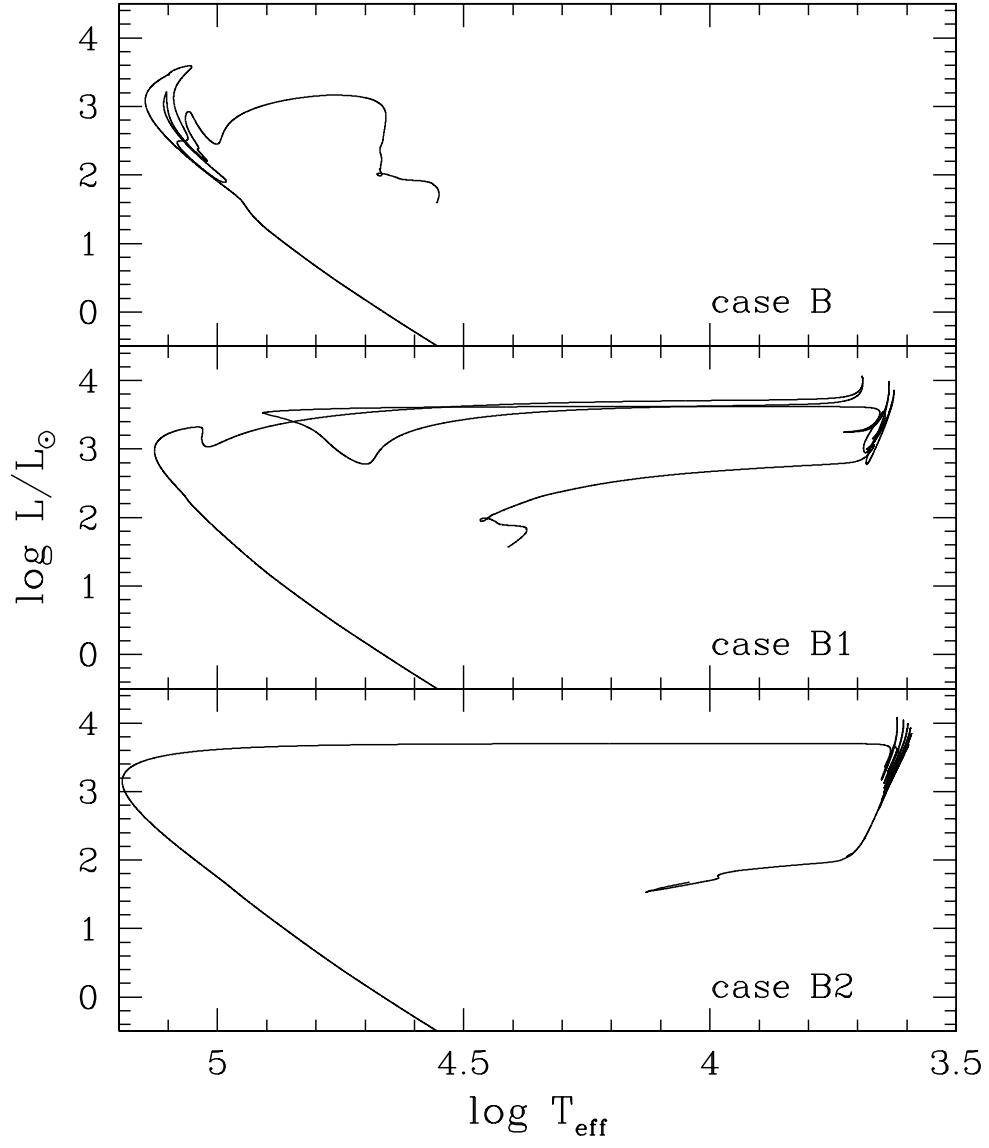


Fig. 2.— Comparison between three different evolutionary tracks leading to a  $0.6 M_{\odot}$  WD (models B, B1 and B2 of table 1).

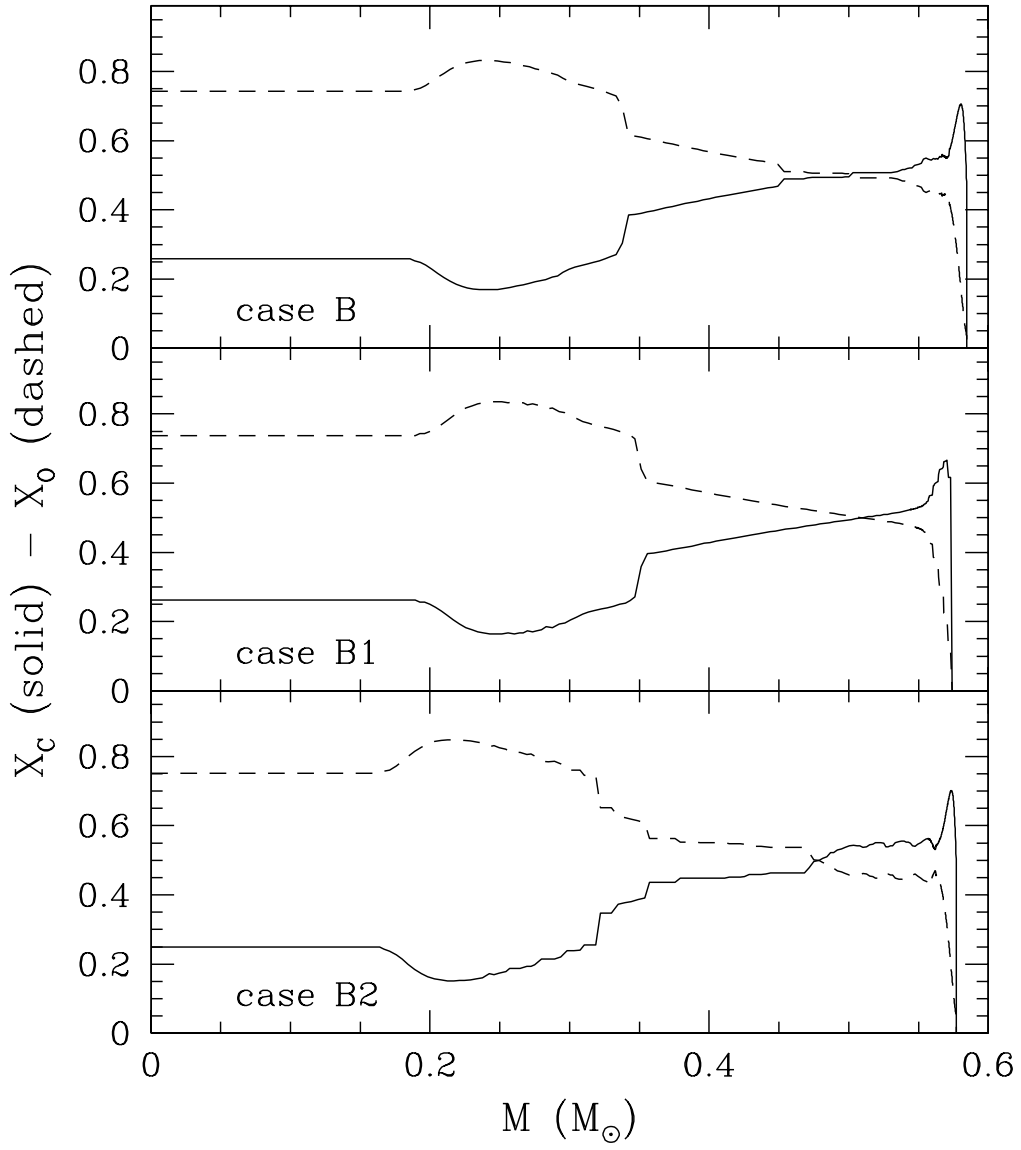


Fig. 3.— Internal profiles of carbon (solid lines) and oxygen (dashed lines) for model B (upper panel), B1 (middle panel) and B2 (lower panel), respectively.

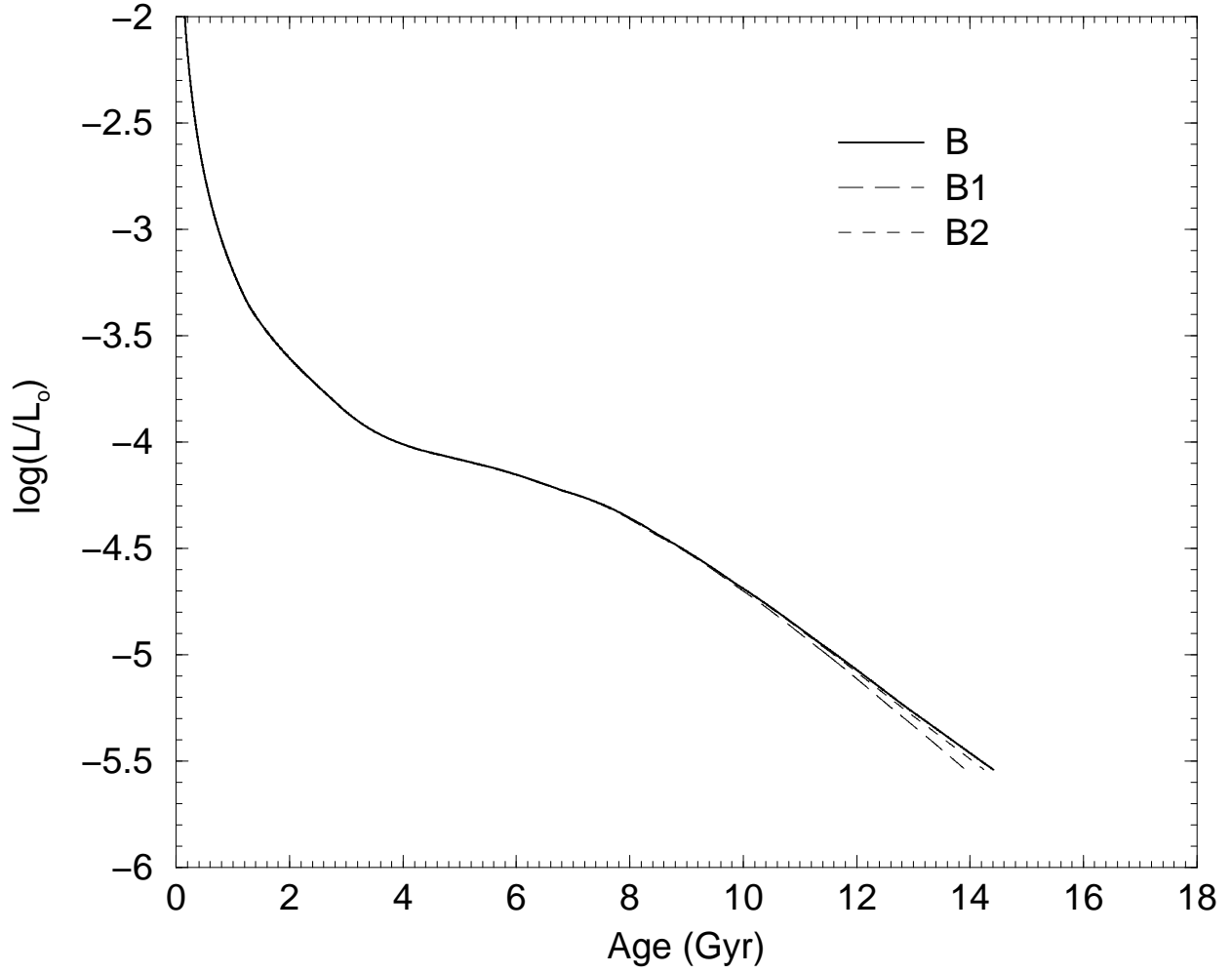


Fig. 4.— Comparison between the cooling sequences for model B (solid line), B1 (long-dashed line) and B2 (dashed), respectively.

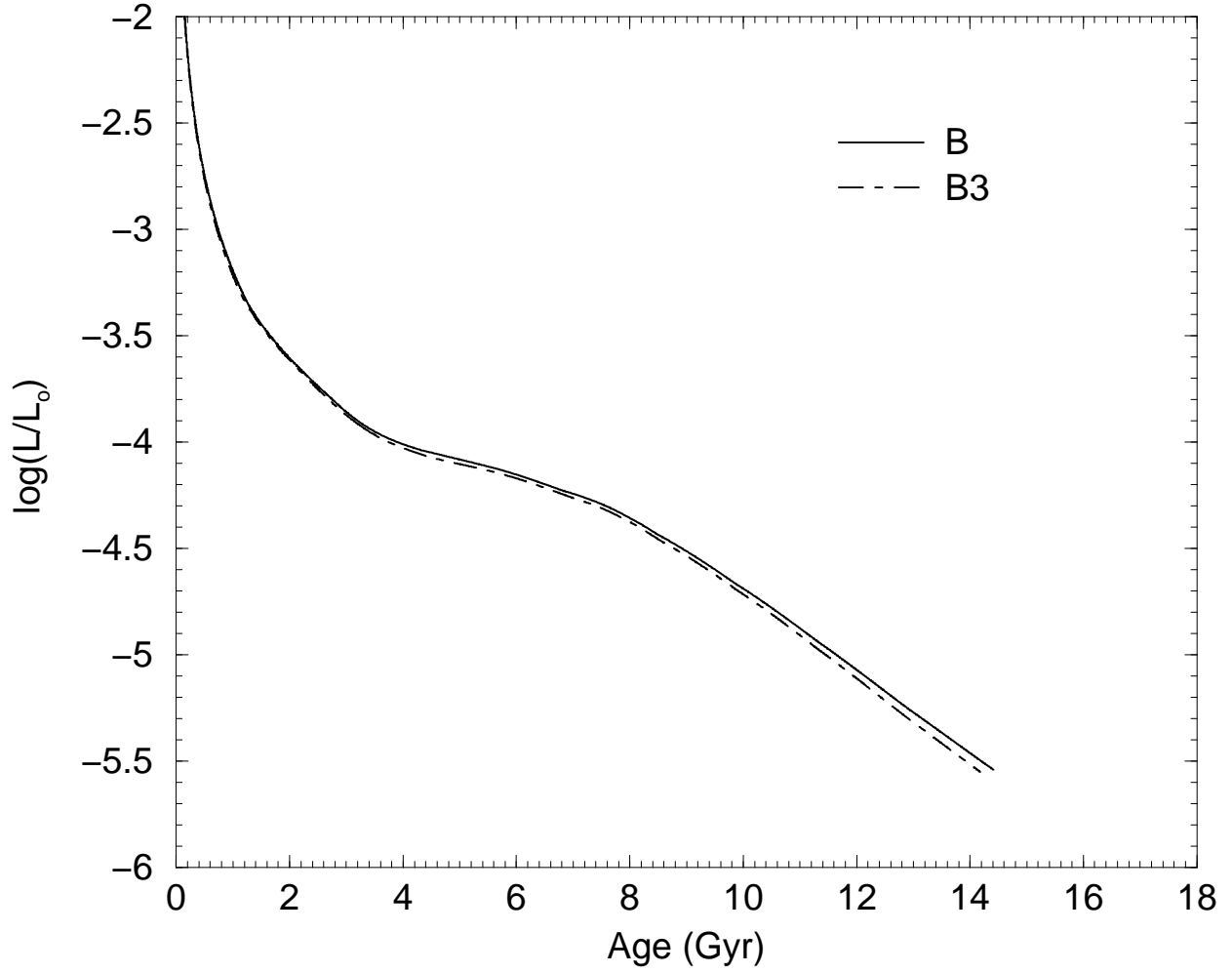


Fig. 5.— Comparison between the cooling sequence obtained for a metal poor progenitor (model B with  $Z=10^{-4}$ ) and a metal rich progenitor (model B3 with  $Z=0.02$ ).

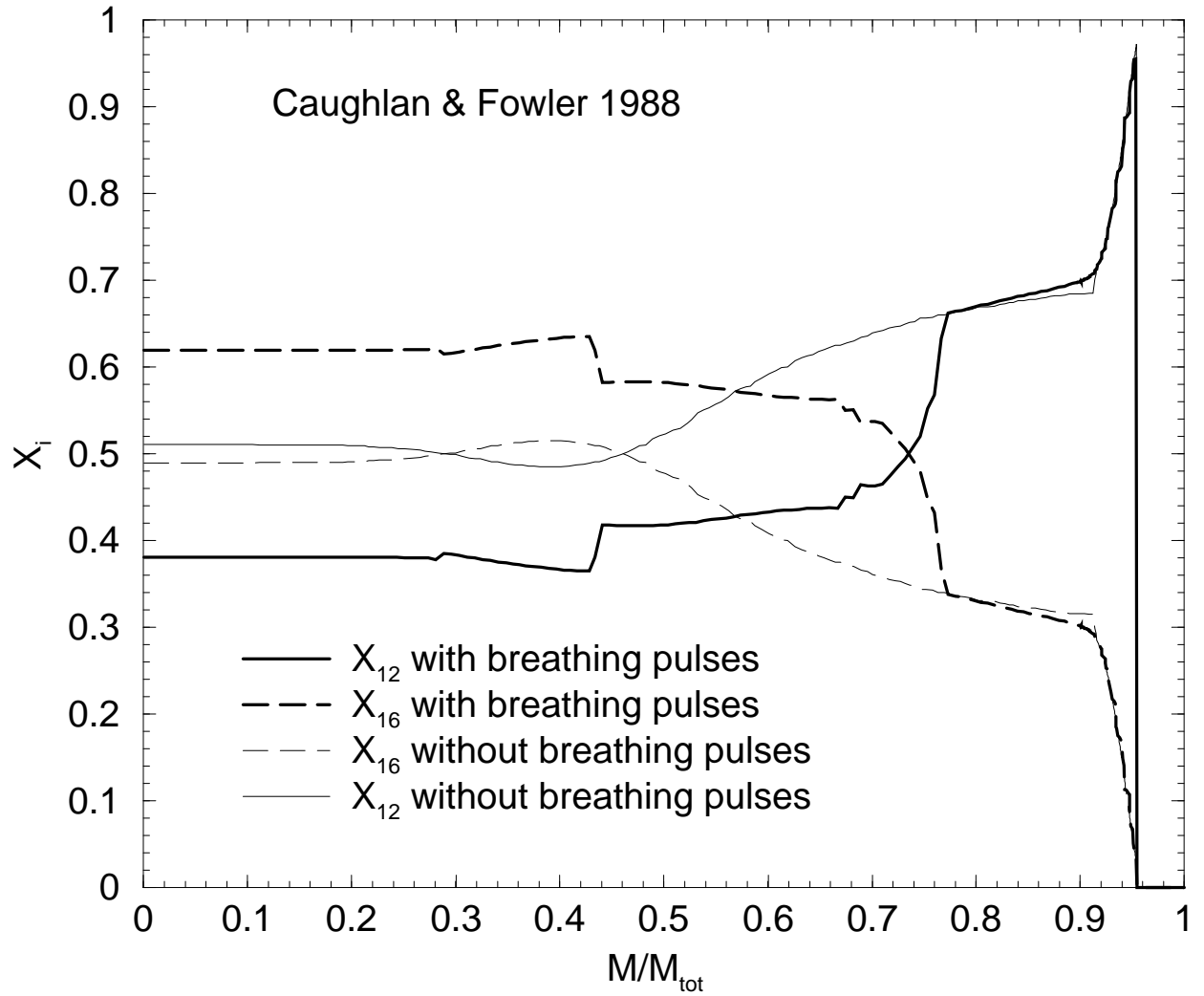


Fig. 6.— Profiles of carbon (solid lines) and oxygen (dashed lines) for the model with (thick lines) and without (thin lines) breathing pulses. In both cases, a low  $^{12}\text{C}(\alpha, \gamma)^{16}\text{O}$  rate (CF88) has been adopted.

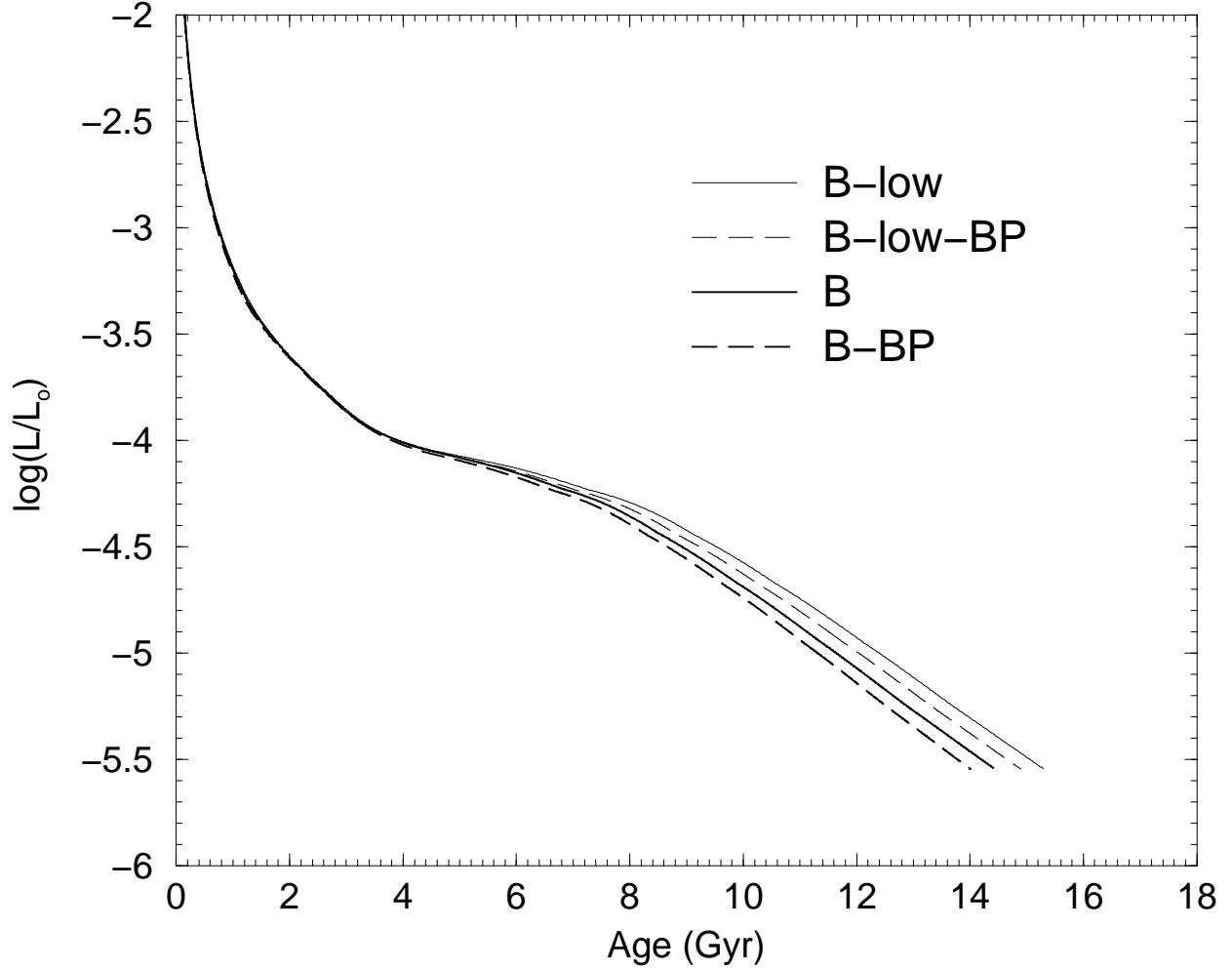


Fig. 7.— Cooling sequences obtained from progenitor evolutions with and without breathing pulses and different  $^{12}\text{C}(\alpha, \gamma)^{16}\text{O}$  rate: no-BPs and CF88 (thin solid line), BPs and CF88 (thin dashed line), no-BPs and CF85 thick solid line, BPs and CF85 (thick dashed line). Note that CF88 and CF85 are representative of a low and a high rate for the  $^{12}\text{C}(\alpha, \gamma)^{16}\text{O}$  (see text).

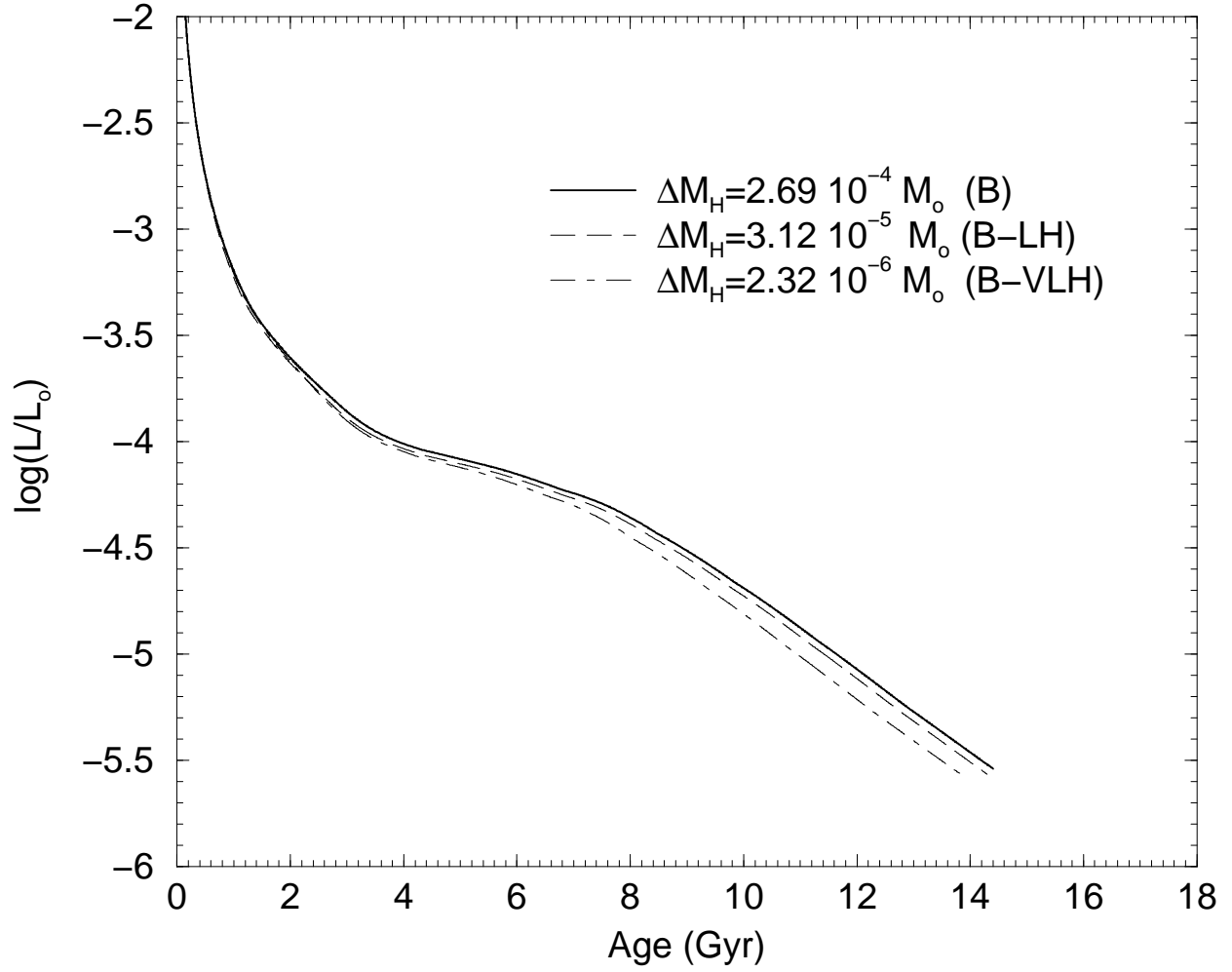


Fig. 8.— Effects, on the cooling sequence, of the extension in mass of the H-rich envelope ( $\Delta M_H$ ).



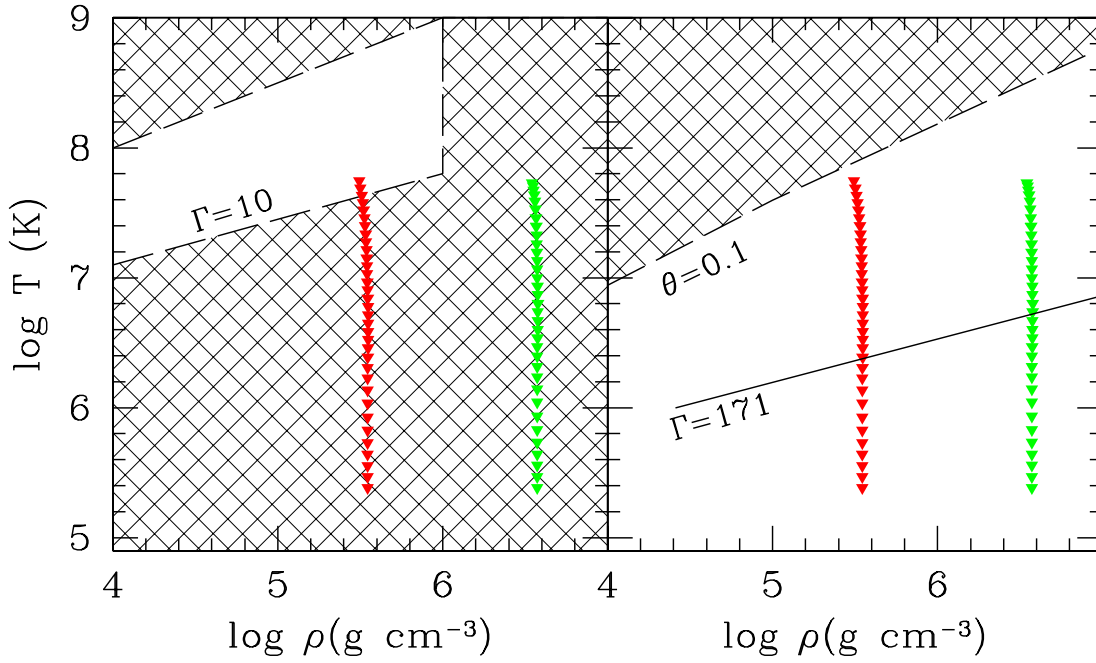


Fig. 9.— Temperature-density diagram for the core. Left panel: hatched area shows where the HL69 conductive opacity are not valid. Right panel: the same but for the I93 conductive opacity. The two series of arrows indicate the evolution of the central conditions and that of the outer border of the core.

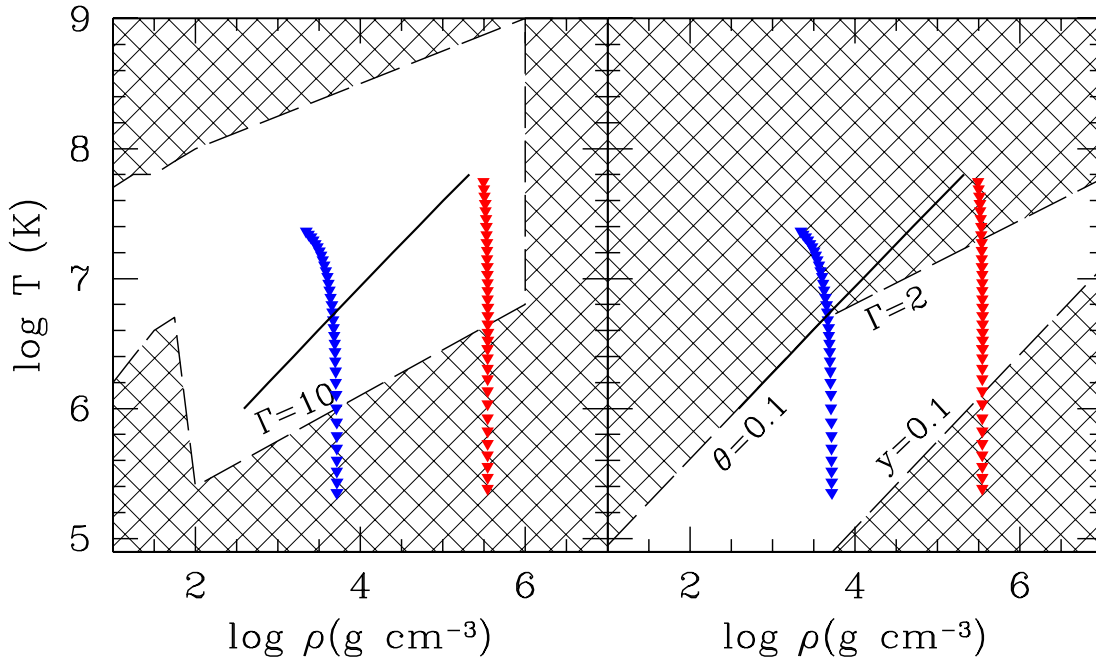


Fig. 10.— Same as figure 9, but for the He-rich mantle. Here, the two series of arrows indicate the evolutions of the physical conditions at the two boundary of the mantle. The thick solid line shows the location of the  $\theta = 0.1$  condition; model B-comb has been obtained by using HL69 above this line and I93 below.

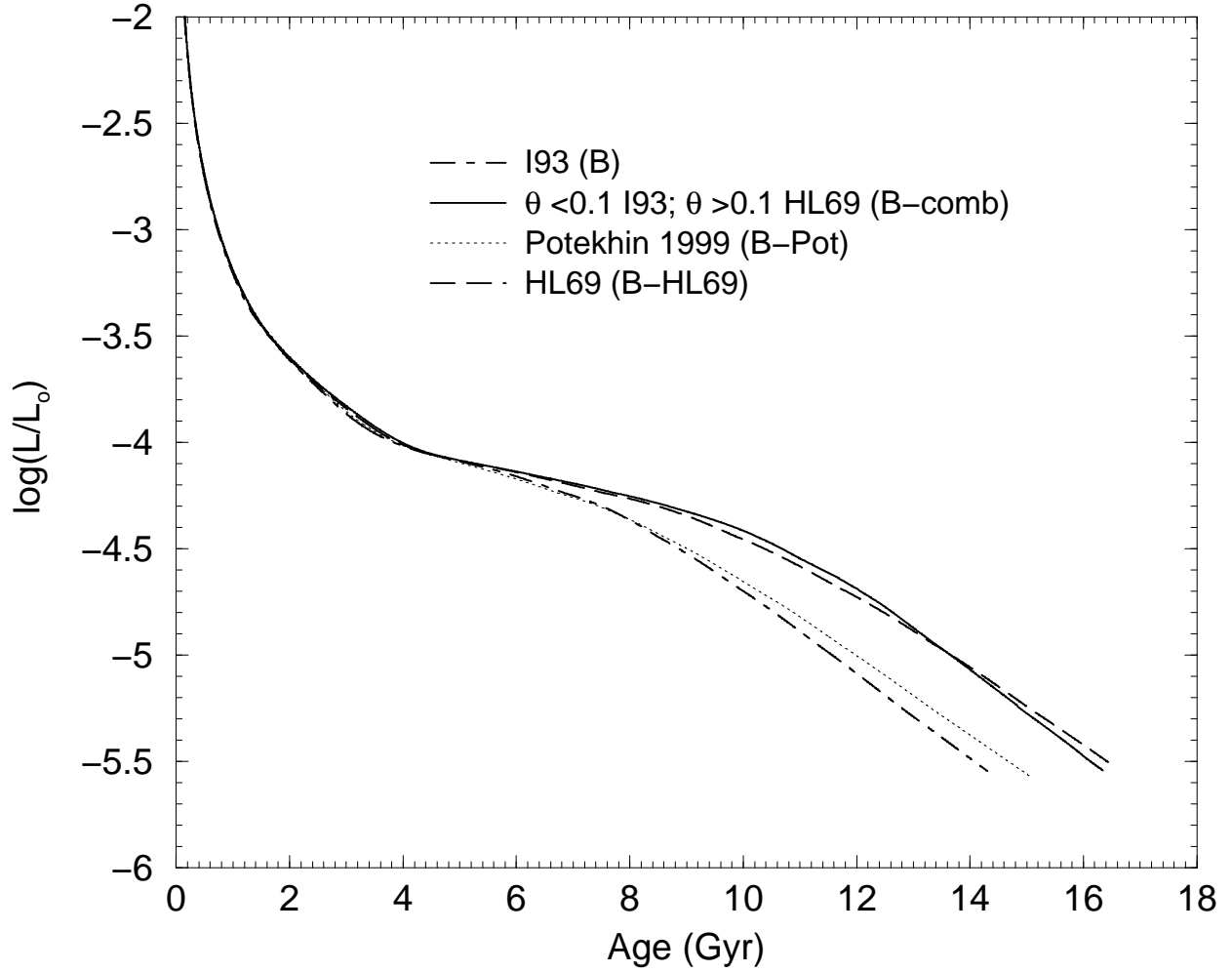


Fig. 11.— Theoretical cooling sequences under different prescriptions for the conductive opacity: I93, Mitake et al. 1984 for the fluid phase and Itoh et al. 1993 for the solid phase (dot-dashed line); HL69, Hubbard & Lampe 1969 (dashed line); I93 for the fully degenerate regime ( $\theta \leq 0.1$ ) and HL69 for the partially degenerate regime (solid line); Potekhin et al. 1999 (dotted line).

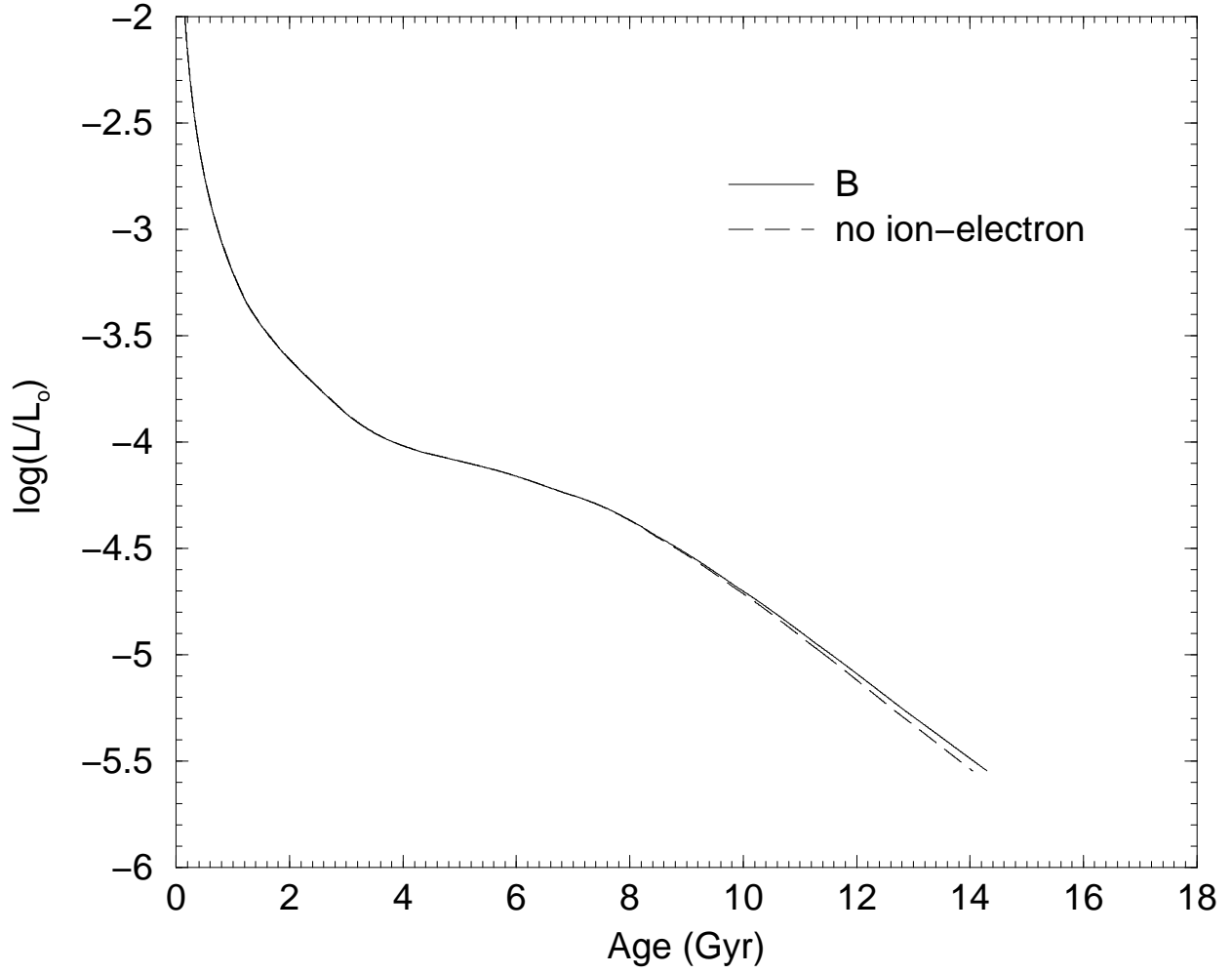


Fig. 12.— Comparison between the cooling sequences computed adopting an EOS with (case B, solid line) and without (dashed line) the ion-electron interaction.

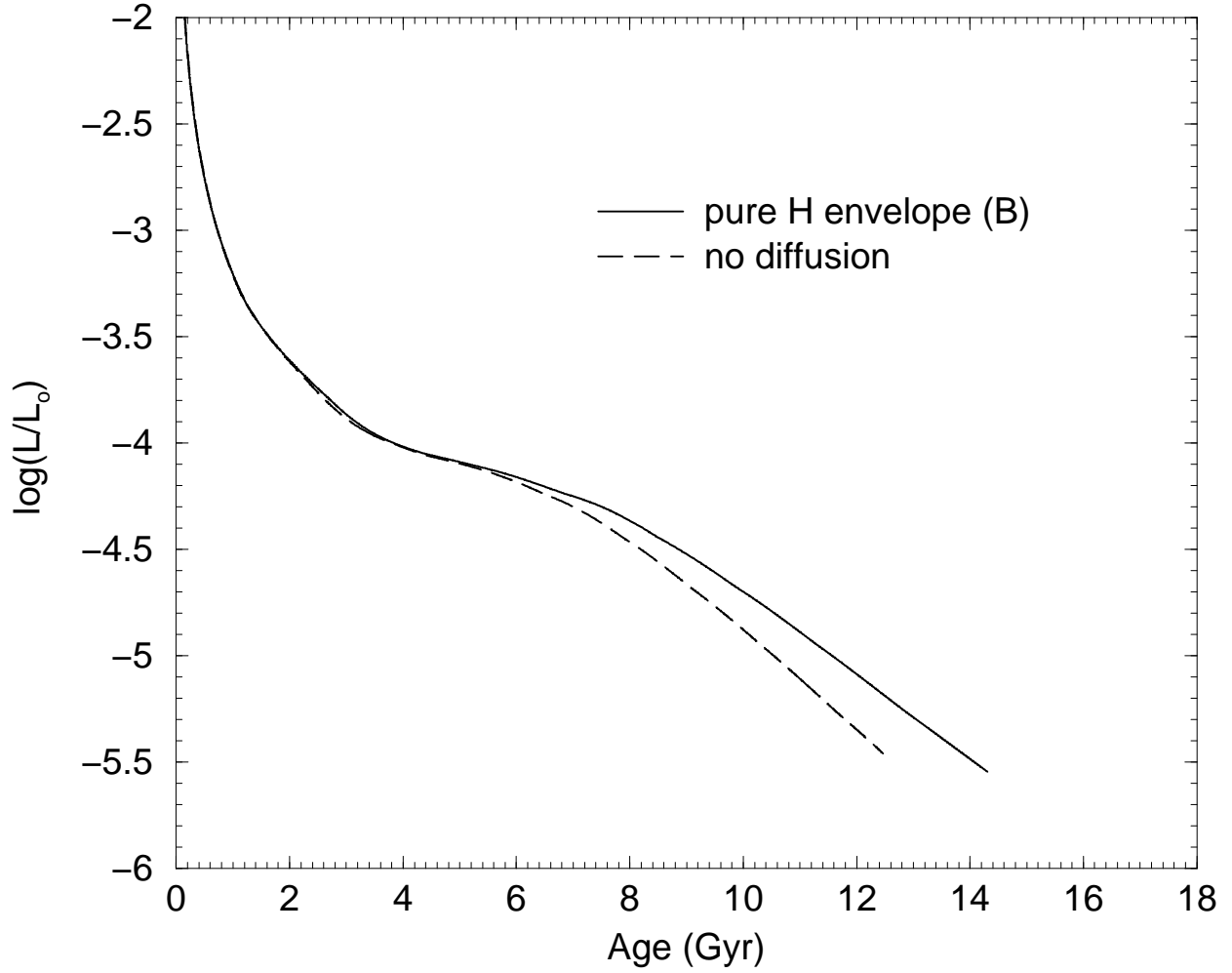


Fig. 13.— Cooling sequences with (solid line) and without (dashed line) the chemical sorting of the H and He layers.

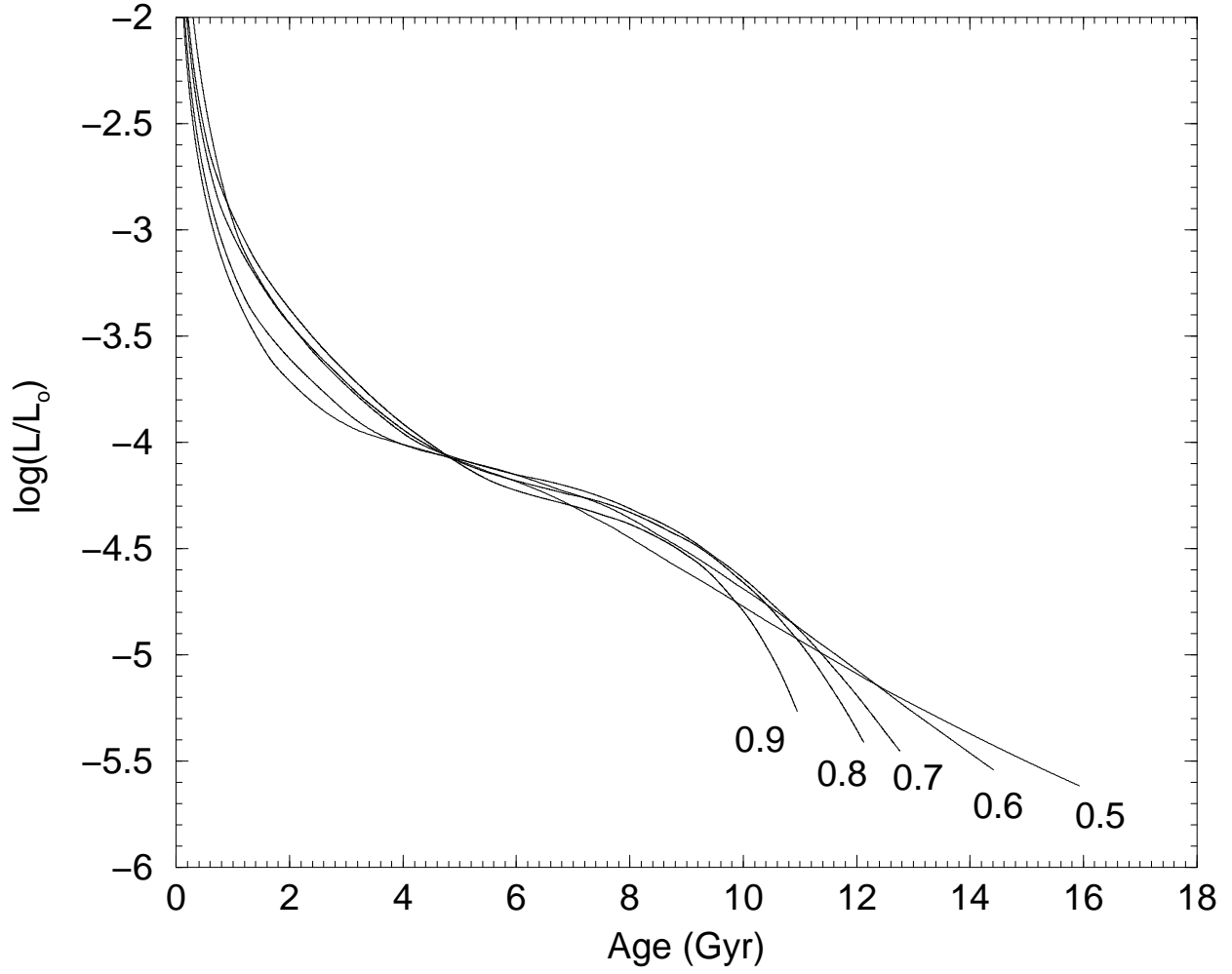


Fig. 14.— Cooling sequences of WDs having mass ranging between 0.5 and 0.9  $M_{\odot}$ .

Table 1.  $0.6 M_{\odot}$  WD: progenitors and cooling

label	$M_{ZAHB}^1$	$Z^1$	$M_{He}^1$	$M_{WD}^2$	$\Delta M_{He}^2$	$\Delta M_H^2$	$X_{12}^c{}^3$	$Q^4$	$\Delta t^5$
B	0.600	0.0001	0.599	0.600	$2.56 \times 10^{-2}$	$2.69 \times 10^{-4}$	0.263	0.573	14.20
B1	0.600	0.0001	0.580	0.600	$1.29 \times 10^{-2}$	$2.53 \times 10^{-4}$	0.258	0.542	13.74
B2	0.640	0.0001	0.515	0.601	$2.03 \times 10^{-2}$	$2.23 \times 10^{-4}$	0.249	0.516	14.05
B3	0.600	0.0200	0.599	0.600	$2.49 \times 10^{-2}$	$8.48 \times 10^{-5}$	0.248	0.509	13.92
B-LH	0.600	0.0001	0.599	0.600	$2.56 \times 10^{-2}$	$3.12 \times 10^{-5}$	0.263	0.573	13.96
B-VLH	0.600	0.0001	0.599	0.600	$2.56 \times 10^{-2}$	$2.32 \times 10^{-6}$	0.263	0.573	13.49
B-BP	0.600	0.0001	0.599	0.600	$2.54 \times 10^{-2}$	$2.64 \times 10^{-4}$	0.151	0.316	13.78
B-low	0.600	0.0001	0.599	0.600	$2.73 \times 10^{-2}$	$2.82 \times 10^{-4}$	0.511	0.483	15.07
B-low-BP	0.600	0.0001	0.599	0.600	$2.71 \times 10^{-2}$	$2.72 \times 10^{-4}$	0.381	0.434	14.65
B-HL69	0.600	0.0001	0.599	0.600	$2.56 \times 10^{-2}$	$2.69 \times 10^{-4}$	0.263	0.573	16.67
B-comb	0.600	0.0001	0.599	0.600	$2.56 \times 10^{-2}$	$2.69 \times 10^{-4}$	0.263	0.573	16.12
B-Pot	0.600	0.0001	0.599	0.600	$2.56 \times 10^{-2}$	$2.69 \times 10^{-4}$	0.263	0.573	14.68
B-noie	0.600	0.0001	0.599	0.600	$2.56 \times 10^{-2}$	$2.69 \times 10^{-4}$	0.263	0.573	13.82
B-nodif	0.600	0.0001	0.599	0.600	$2.56 \times 10^{-2}$	$2.69 \times 10^{-4}$	0.263	0.573	12.63

<sup>1</sup>Start parameters (ZAHB): mass ( $M_{ZAHB}[M_{\odot}]$ ), metallicity ( $Z$ ), He core mass ( $M_{He}[M_{\odot}]$ )

<sup>2</sup>WD parameters: total mass ( $M_{WD}[M_{\odot}]$ ), He mass ( $\Delta M_{He}[M_{\odot}]$ ) and H mass ( $\Delta M_H[M_{\odot}]$ )

<sup>3</sup>Mass fraction of carbon at the center of the WD

<sup>4</sup>Ratio between the mass of the innermost homogeneous region and the total WD mass

<sup>5</sup>age (in Gyr) at the faint end, namely the time necessary to cool down from  $\log(L/L_{\odot}) = 0$  to  $\log(L/L_{\odot}) = -5.5$ .

Table 2. WD models with different mass

label	$M_{WD}^1$	$\Delta M_{He}^2$	$\Delta M_H^3$	$X_{12}^c{}^4$	$Q^5$	$\Delta t^6$
A	0.500	$4.62 \times 10^{-2}$	$4.24 \times 10^{-4}$	0.221	0.571	15.00
B	0.600	$2.56 \times 10^{-2}$	$2.69 \times 10^{-4}$	0.263	0.573	14.20
C	0.700	$8.92 \times 10^{-3}$	$1.27 \times 10^{-4}$	0.294	0.560	12.90
D	0.800	$5.85 \times 10^{-3}$	$6.15 \times 10^{-5}$	0.302	0.529	12.31
E	0.900	$3.04 \times 10^{-3}$	$3.87 \times 10^{-5}$	0.309	0.492	11.32

<sup>1</sup>WD mass ( $M_\odot$ )

<sup>2</sup>He mass ( $M_\odot$ )

<sup>3</sup>H mass ( $M_\odot$ )

<sup>4</sup>Mass fraction of carbon at the center of the WD

<sup>5</sup>Ratio between the mass of the innermost homogeneous region and the total WD mass

<sup>6</sup>age (in Gyr) at the faint end, namely the time necessary to cool down from  $\log(L/L_\odot) = 0$  to  $\log(L/L_\odot) = -5.5$ .